

DEVELOPMENT OF HYALURONIC ACID-BASED NANOGEL PLATFORM FOR IMPROVED
STABILITY AND POLYVALENT LIGAND DISPLAY OF POLY(I:C) AS AN EFFECTIVE
IMMUNOSTIMULATORY ADJUVANT IN CANCER IMMUNOTHERAPY



A Thesis Submitted in Partial Fulfillment of the Requirements
for the Degree of Master of Science in Pharmaceutical Sciences and Technology

Common Course

FACULTY OF PHARMACEUTICAL SCIENCES

Chulalongkorn University

Academic Year 2020

Copyright of Chulalongkorn University

การพัฒนาแพลตฟอร์มนาโนเจลที่สร้างจากกรดไฮยาลูโรนิกเพื่อเพิ่มเสถียรภาพและการแสดงออกของ
ลิแกนด์โพลีวาเลนต์ของโพลี(ไอ:ซี) ในการเป็นตัวเสริมเพื่อกระตุ้นภูมิคุ้มกันที่มีประสิทธิภาพในการ
บำบัดมะเร็งด้วยภูมิคุ้มกัน



วิทยานิพนธ์นี้เป็นส่วนหนึ่งของการศึกษาตามหลักสูตรปริญญาวิทยาศาสตรมหาบัณฑิต
สาขาวิชาเภสัชศาสตร์และเทคโนโลยี ไม่สังกัดภาควิชา/เทียบเท่า
คณะเภสัชศาสตร์ จุฬาลงกรณ์มหาวิทยาลัย
ปีการศึกษา 2563
ลิขสิทธิ์ของจุฬาลงกรณ์มหาวิทยาลัย

Thesis Title DEVELOPMENT OF HYALURONIC ACID-BASED NANOGEL
PLATFORM FOR IMPROVED STABILITY AND POLYVALENT
LIGAND DISPLAY OF POLY(I:C) AS AN EFFECTIVE
IMMUNOSTIMULATORY ADJUVANT IN CANCER
IMMUNOTHERAPY

By Miss Nararat Kotcharat

Field of Study Pharmaceutical Sciences and Technology

Thesis Advisor Assistant Professor Jittima Luckanagul, Ph.D.

Accepted by the FACULTY OF PHARMACEUTICAL SCIENCES, Chulalongkorn
University in Partial Fulfillment of the Requirement for the Master of Science

..... Dean of the FACULTY OF
PHARMACEUTICAL SCIENCES
(Assistant Professor RUNGPETCH SAKULBUMRUNGSIL,
Ph.D.)

THESIS COMMITTEE

..... Chairman
(Assistant Professor NARUEPORN SUTANTHAVIBUL, Ph.D.)

..... Thesis Advisor
(Assistant Professor Jittima Luckanagul, Ph.D.)

..... Examiner
(Associate Professor WARANYOO PHOOLCHAROEN, Ph.D.)

..... External Examiner
(Apirada Sucontphunt, Ph.D.)

นรรัตน์ คชรัตน์ : การพัฒนาแพลตฟอร์มนาโนเจลที่สร้างจากกรดไฮยาลูโรนิกเพื่อเพิ่มเสถียรภาพและการแสดงออกของลิแกนด์โพลีวาเลนต์ของโพลี(ไอ:ซี) ในการเป็นตัวเสริมเพื่อกระตุ้นภูมิคุ้มกันที่มีประสิทธิผลในการบำบัดมะเร็งด้วยภูมิคุ้มกัน. (

DEVELOPMENT OF HYALURONIC ACID-BASED NANOGEL PLATFORM FOR IMPROVED STABILITY AND POLYVALENT LIGAND DISPLAY OF POLY(I:C) AS AN EFFECTIVE IMMUNOSTIMULATORY ADJUVANT IN CANCER

IMMUNOTHERAPY) อ.ที่ปรึกษาหลัก : ผศ. ภาณุ.ดร.จิตติมา ลักนากุล

งานวิจัยนี้มีจุดมุ่งหมายเพื่อพัฒนาสูตรนาโนเจลโดยใช้พอลิเมอร์ที่ได้จากธรรมชาติได้แก่กรดไฮยาลูโรนิก (hyaluronic acid) ซึ่งเป็นวัสดุย่อยสลายทางชีวภาพสำหรับการนำส่งสารเสริมภูมิคุ้มกัน Polyinosinic: polycytidylic acid (poly (I: C)) หรือโพลี(ไอ:ซี) ได้รับการรับรองจากสำนักงานคณะกรรมการอาหารและยา (Food and Drug Administration) ว่าเป็นสารเสริมภูมิคุ้มกันที่ได้รับการรับรองว่ามีแนวโน้มสำหรับการกระตุ้น Toll-Like Receptor 3 (TLR3) อย่างไรก็ตาม โพลี(ไอ:ซี) มีข้อจำกัดด้านความเสถียรและการสลายตัวจากการย่อยของเอนไซม์ในซีรัม จึงมีความจำเป็นในการบริหารยาปริมาณที่สูงนำมาสู่การเกิดผลข้างเคียงในที่สุด ดังนั้นเพื่อเพิ่มเสถียรภาพของโพลี(ไอ:ซี) จึงได้ออกแบบอนุภาคนาโนโดยใช้กรดไฮยาลูโรนิกเป็นโครงสร้างหลักในการประกอบขึ้นเองของพอลิเมอร์ (self-assembly) และการต่อกิ่งพอลิเมอร์โดยใช้สารเชื่อมต่อ (EDC/NHS) ผ่านการประกอบขึ้นของหมู่เอไมด์ระหว่าง poly (N-isopropylacrylamide) (pNIPAM) และกรดไฮยาลูโรนิก จากนั้นยืนยันการต่อกิ่งของพอลิเมอร์ (HA-g-pNI) โดยการวิเคราะห์สเปกตรัมของ ^1H NMR สำหรับการรวมกันทางกายภาพของกรดนิวคลีอิกและนาโนเจลถูกดำเนินการขึ้นโดยวิธีการบ่มโดยใช้ความเข้มข้นของโพลี(ไอ:ซี) เท่ากับ 0.2, 1 และ 10 ($\mu\text{g} / \text{mL}$) ในสูตรนาโนเจลที่ใช้ 0.1, 0.25 และ 0.5 (% w/v) ของ HA-g-pNI ในการฟอร์มตัวของอนุภาคจากผลการทดลองพบว่าขนาดเฉลี่ย การกระจายของขนาดอนุภาคและประจุบนพื้นผิวของอนุภาคนาโนเจลถูกตรวจสอบโดยการกระเจิงของแสงแบบไดนามิก (DLS) ฐานวิทยาของอนุภาคถูกตรวจสอบโดยกล้องจุลทรรศน์อิเล็กตรอนแบบส่องผ่าน (TEM) ผลลัพธ์แสดงให้เห็นว่า HA-g-pNI ที่มีระดับการ graft เท่ากับ 4% อนุภาคนาโนเจลมีลักษณะคล้ายทรงกลมอยู่ในช่วงไมโครเมตรและแสดงค่าศักย์ไฟฟ้าของพื้นผิวอนุภาค (zeta-potential) เป็นลบ นอกจากนี้ยังพบว่าอนุภาคที่โหลดโพลี(ไอ:ซี) มีขนาดและ PDI ลดลงอย่างมีนัยสำคัญเมื่อทำการบ่มอย่างต่อเนื่อง ซึ่งแสดงให้เห็นสาขาวิชา เกษศาสตร์และเทคโนโลยี ลายมือชื่อนิสิต
ปีการศึกษา 2563 ลายมือชื่อ อ.ที่ปรึกษาหลัก

6176102733 : MAJOR PHARMACEUTICAL SCIENCES AND TECHNOLOGY

KEYWORD: Adjuvant delivery cancer Immunotherapy hyaluronic acid nanogels
poly(I:C)

Nararat Kotcharat : DEVELOPMENT OF HYALURONIC ACID-BASED NANO GEL PLATFORM FOR IMPROVED STABILITY AND POLYVALENT LIGAND DISPLAY OF POLY(I:C) AS AN EFFECTIVE IMMUNOSTIMULATORY ADJUVANT IN CANCER IMMUNOTHERAPY. Advisor: Asst. Prof. Jittima Luckanagul, Ph.D.

The aim of this research was to develop a nanogel formulation-based on modified natural polymer, hyaluronic acid (HA), as a biodegradable material for adjuvant delivery. Polyinosinic:polycytidylic acid (poly(I:C)) have been approved by FDA as a promising adjuvant candidate for the TLR3 (Toll-Like Receptor 3) activation. However, it suffers from being poor stability and is subjected to rapid enzymatic hydrolysis in serum, so that it requires high administered dose leading to adverse effects. To augment the adjuvant stability and protection from the degradation, the nano-particulate carriers were herein designed with self-assembly of HA scaffold grafted with poly (N-isopropylacrylamide), or pNIPAM. The grafting was processed through amide formation using the coupling agent (EDC/NHS). ¹H NMR was carried out to confirm the modified products (HA-g-pNI). The physical incorporation of the nucleic acid into the grafted HA nanogel was achieved by incubation method with the poly(I:C) concentrations of 0.2, 1, and 10 (μ g/mL) in formulations by using 0.1, 0.25, and 0.5 (% w/v) of HA-g-pNI to form the nanogel particles. The mean size, size distribution and surface charge of the nanogel particles were determined by dynamic light scattering (DLS). The particle morphology was investigated by transmission electron microscopy (TEM). Results demonstrated that HA-g-pNI with a 4 % degree of substitution were formed into nearly spherical nanogel particles with the size of approximately submicron range. The particles presented a negative value in zeta-

Field of Study: Pharmaceutical Sciences Student's Signature
and Technology

Academic Year: 2020

Advisor's Signature

ACKNOWLEDGEMENTS

This research could not be accomplished without the support from the faculty of Pharmaceutical Sciences, Chulalongkorn University. In particular, I would like to express the deepest appreciation to my thesis supervisor, Assistant Professor Jittima Luckanagul, Ph.D., Department of Pharmaceutics and Industrial Pharmacy, Faculty of Pharmaceutical Sciences, Chulalongkorn University for her opportunity, superior advice, and support throughout the thesis operation.

Next, I would like to thank all the people whose assistances for my project, including staffs and all friends at the Faculty of Pharmaceutical Sciences, Chulalongkorn University, especially I most gratefully acknowledge my mentor, Penpimon Charoenkanburkang, M.Sc. and also Sirikool Thamniem, M.Sc. from the Department of Pharmaceutics and Industrial Pharmacy, Faculty of Pharmaceutical Sciences, Chulalongkorn University for their training and suggestions.

Also, I would like to show appreciation to Chawanphat Muangnoi, Ph.D. (Cell and Animal Model Unit, Institute of Nutrition, Mahidol University) for her assistance with RAW 264.7 macrophage cell lines. Besides, I am grateful for the help from Associate Professor Waranyoo Phoolcharoen, Ph.D. and also Kaewta Rattanapisit, Ph.D. from Department of Pharmacognosy and Pharmaceutical Botany, Faculty of Pharmaceutical Sciences, Chulalongkorn University in training gel electrophoresis.

The authors would like to show gratitude to the Research Instrument Center of Faculty of Pharmaceutical Sciences, Chulalongkorn University for providing research facility. This research was supported partly by Graduate School Thesis Grant and Chulalongkorn Academic Advancement into its Second Century (CUAASC) Project.

Finally, I am appreciative of my family and my parents for all support and encouragement throughout the period of this research.

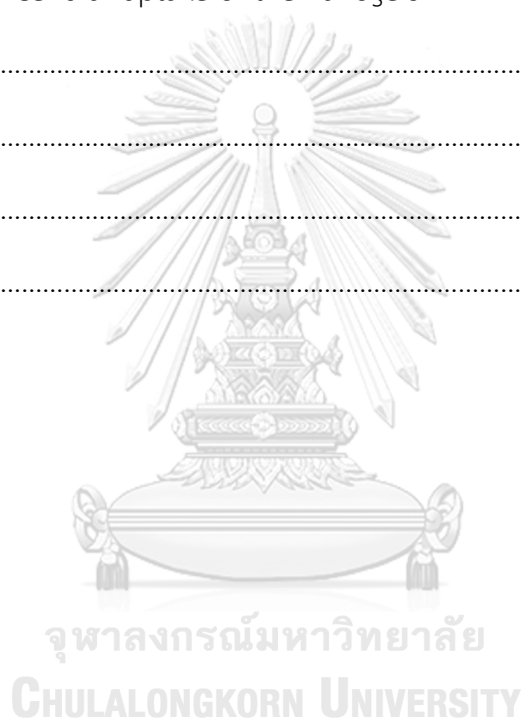
Nararat Kotcharat

TABLE OF CONTENTS

	Page
ABSTRACT (THAI).....	iii
ABSTRACT (ENGLISH).....	iv
ACKNOWLEDGEMENTS	v
TABLE OF CONTENTS	vi
LIST OF TABLE	1
LIST OF FIGURES	1
CHAPTER I.....	1
INTRODUCTION.....	1
CHAPTER II.....	3
LITERATURE REVIEWS	3
1. Cancer vaccines-based immunotherapy.....	3
1.1 Components of cancer vaccination.....	3
1.2 Development of vaccine adjuvant	3
2. Poly(I:C) as an immunostimulatory adjuvant	4
2.1 Signaling induced by poly(I:C).....	4
2.2 The major challenges of poly(I:C) in clinical trials.....	6
2.3 Derivative poly(I:C) in clinical study.....	6
3. Overcoming poly(I:C) limitations by designing the particulate systems.....	6
4. Nanocarriers as ligand delivery	7
5. Nanogels.....	8
5.1 Nanogels-based delivery systems.....	8

5.2	Advantages of nanogels	8
5.3	Nanogels for the poly(I:C) delivery	9
6.	Hyaluronic acid.....	11
6.1	Hyaluronic acid targeting to CD44 receptor.....	12
6.2	Nanogel based on hyaluronic acid	13
7.	Poly (N-isopropylacrylamide)	14
CHAPTER III.....		16
METHODOLOGY.....		16
Chemicals and materials		16
Methods.....		16
1.	Synthesis of pNIPAM grafted hyaluronic acid.	16
2.	Preparation of HA-g-pNI nanogel and nucleic acid loading.....	17
3.	Characterization of adjuvant-free and poly(I:C) nanogels.....	18
4.	Formation of poly(I:C)-incorporated HA-g-pNI nanogels.....	18
5.	<i>In vitro</i> physiological stability of poly(I:C) within nanogels.....	19
6.	Cell viability assay	19
7.	<i>In vitro</i> cellular uptake study of poly(I:C).....	20
8.	Statistical analysis.....	21
CHAPTER IV		22
RESULTS AND DISCUSSIONS		22
I.	Synthesis and characterization of pNIPAM grafted HA.....	22
II.	Physical characterization of adjuvant-free nanogels.....	23
III.	Preparation and characterization of the adjuvant-loaded hyaluronic acid nanogels	27

IV. Nanogel morphology	29
V. Evaluation of the lower critical solution temperature of nanogels	31
VI. Poly(I:C) formation assessment	33
VII. Physiological stability of poly(I:C)-loaded HA-g-pNI nanogels against serum degradation	35
VIII. Cell viability by RAW 264.7 macrophage cell lines	36
IX. The study of cellular uptake of the nanogels	39
CHAPTER V	42
CONCLUSIONS	42
REFERENCES	2
VITA.....	4



LIST OF TABLE

	Page
Table 1 : Research plan 1Physical properties of the HA-g-pNI nanogels and the poly(I:C) loaded nanogels in each formulation measured by DLS.....	25



LIST OF FIGURES

	Page
Figure 1 : Scheme of the activation of the immune system against pathogen after PAMP-PRR interaction from the pathogen entry into the cell.....	4
Figure 2 : Illustration of the poly(I:C) structure.	5
Figure 3 : Schematic of chitosan nanoparticles encapsulating an adjuvant and OVA as an antigen model, and the nanoparticle prepared by ionic complex	11
Figure 4 : Illustration of the structure of hyaluronic acid.	12
Figure 5 : The structure of poly(N-isopropylacrylamide) (pNIPAM).	14
Figure 6 : Schematic illustration of the procedures for the synthesis of pNIPAM grafting polymer on HA as a backbone through EDC/NHS coupling reaction	22
Figure 7 : ¹ H NMR spectra of pNIPAM-grafted hyaluronic acid (HA-g-pNI) with 4% degrees of modification..	22
Figure 8 : Physical properties of HA-g-pNI nanogels and adjuvant-loaded HA-g-pNI nanogels.....	26
Figure 9 : The particle morphology of assembled HA-g-pNI nanogels with 4% degree of grafting measured by TEM.	30
Figure 10 : The LCST profile of naked nanogel in three different concentrations of HA-g-pNI polymer.....	32
Figure 11 : The LCST profile of poly(I:C)-loaded nanogel formulations in two different concentrations of HA-g-pNI polymer forming gel.....	33
Figure 12 : Agarose gel electrophoresis represents the characteristics of the poly(I:C) incorporated within the HA-g-pNI nanogels in each formulations (a). The poly(I:C) association in the assembled nanogels was evaluated using agarose gel by incubating poly(I:C) nanogel with hyaluronidase solution (b).....	35

- Figure 13 : Comparative gel electrophoresis of the physiological stability of soluble poly(I:C) (d) and poly(I:C)-loaded HA-g-pNI (a, b and c) in the presence of nuclease in FBS. 36
- Figure 14 : Viability of RAW 264.7 macrophages treated with different formulations of HA-g-pNI nanogels with and without poly(I:C) as well as comparable poly(I:C) solutions after 24 hrs of incubation for PrestoBlue assay..... 38
- Figure 15 : Cellular uptake study of HA-g-pNI nanogels with- and without poly(I:C) by Raw 264.7 macrophages..... 41



CHAPTER I

INTRODUCTION

The aim of current researches in the field of cancer immunotherapy was to develop vaccination in the treatment of cancer (1). Therapeutic vaccines have been popularly used in clinical trials by driving the host's immune systems to fight with existing cancer. However, most traditional vaccines have often suffered from poorly immunogenic and rapidly degraded, affecting therapeutic efficacy in the patients. Therefore, this calls for efficient carriers and potent immunostimulatory adjuvants that is an alternative way, which could help the induction of antitumor immune responses and while reducing the amount of antigen used to improve therapeutic efficacy.

As several cascades, double-stranded RNA, polyinosinic:polycytidylic acid (poly(I:C)), have been approved by FDA as a promising adjuvant candidate for the strong activation of TLR3 (Toll-Like Receptor 3) danger signal. Many researchers have widely used them for co-administration with traditional vaccination in clinical trials as they can be potent immunostimulants through humoral immune response leading to indirectly cell-mediated immunity against cancer cells (2). However, there is a critical limitation in clinical from poor stability and subject to short half-life in the serum (3). The current challenges are for improving both the stability and safety in the critical issues of poly(I:C), which can be overcome by the development of efficient adjuvant delivery systems, aiming for the efficient and safe cancer vaccination.

As an alternative, nanotechnology-based biocompatible nanogels is currently being studied as a novel innovation that had the potential to overcome the several limitations of the adjuvants. Firstly, nanogels can protect payloads against rapid degradation, whereas its polyvalency property (e.g., specific affinity and bindings, strong interaction between ligand-receptor bindings, high surface area, and high localization

of ligands or adjuvants) can have influence on the enhanced cellular uptake (4). Importantly, these properties can regulate the bioavailability of the bioactive molecule and the drug release profile (5). Moreover, the drug release can be controlled by modifying the stimuli-responsive polymers within the assembled nanogels, which is one critical aspect of the drug delivery systems.

There are 3 major parts in this study; 1) polysaccharide polymer syntheses and grafting with a thermoresponsive polymer; 2) the self-assembled nanogel with the adjuvant encapsulation; 3) their cellular uptake studies. The hyaluronic acid (HA), a natural polysaccharide polymer was used as a scaffold to be assembled with poly-(N-isopropylacrylamide) (pNIPAM) as a thermal sensitive polymer grafting process. The obtained sub-micron hydrogels were used to encapsulate the poly(I:C) providing a novel nanogel. Then, the studies on the pharmaceutical aspect for cancer immunotherapy were performed. The characteristics of poly(I:C) nanogel, such as the physical properties and responsive behavior of the particles were investigated. The physiological stability of the adjuvant-loaded nanogels were assessed as well as the cell viability study to confirm their safety, following by the study of cellular uptake efficiency by RAW 264.7 macrophages.

The successful development of the nanogel platforms for the delivery of effective immunostimulatory adjuvant, poly(I:C), were used as a clinical application for enhanced immune response levels to destroy cancer cells and minimize the toxicity of the adjuvant in the patients. Moreover, a novel hybrid-nanogel platform will lead to advanced materials that can be applied to the delivery of other biomacromolecules for biomedical applications.

CHAPTER II

LITERATURE REVIEWS

1. Cancer vaccines-based immunotherapy

Immunotherapy has been used as an approach alternatively in potential therapeutic cancers (1), for instance of an attractive cancer vaccination based on dendritic cells could modulate the host's immune system to induce effective anti-tumor responses. As a result of the immune evasive strategies of cancer whether or inactive existing tumor antigens in the patients, causing the immune system cannot eliminate these tumor cells. Therefore, cancer vaccination has raised the hope for unleashing patients' immune system to destroy tumors.

1.1 Components of cancer vaccination

There are two parts of components of the cancer vaccination; 1) tumor-associated antigens (TAAs) since these TAAs often poorly immunogenic and therefore administration of additional immunostimulatory adjuvants are needed; 2) potential adjuvants that are important to induce an innate immunity and lead to potent of cell-mediated immune response including cytotoxic T lymphocytes (CTLs), phagocytes, and cytokine production that are critical to combat against tumors.

1.2 Development of vaccine adjuvant

For the development of cancer vaccines, the immunostimulatory molecules or adjuvants are known as pathogen-associated molecular patterns (PAMPs), which widely used in clinical trials such as single- and double-stranded RNA, etc. Normally, PAMPs are recognized by pattern recognition receptor (PRR) that is investigated as Toll-like receptors (TLRs) expressing on several immune cells, including dendritic cells, macrophages and even on non-immune cells e.g., fibroblasts and epithelial cells (6).

PAMPs can provide danger signals on APCs by increasing antigen presentation through major histocompatibility complex (MHC)-restricted classes I and II, producing the cytokines, and thus enhancing immune response. Consequently, PAMPs have regarded as immune stimulation. Recently, most researches emphasize the importance of the design and development of cancer vaccine adjuvants as security while have good clinical efficiency. Although the number of vaccine adjuvants has successful in the animal models, there are few of both safe and effective cancer vaccines that indicate actual clinical benefits.

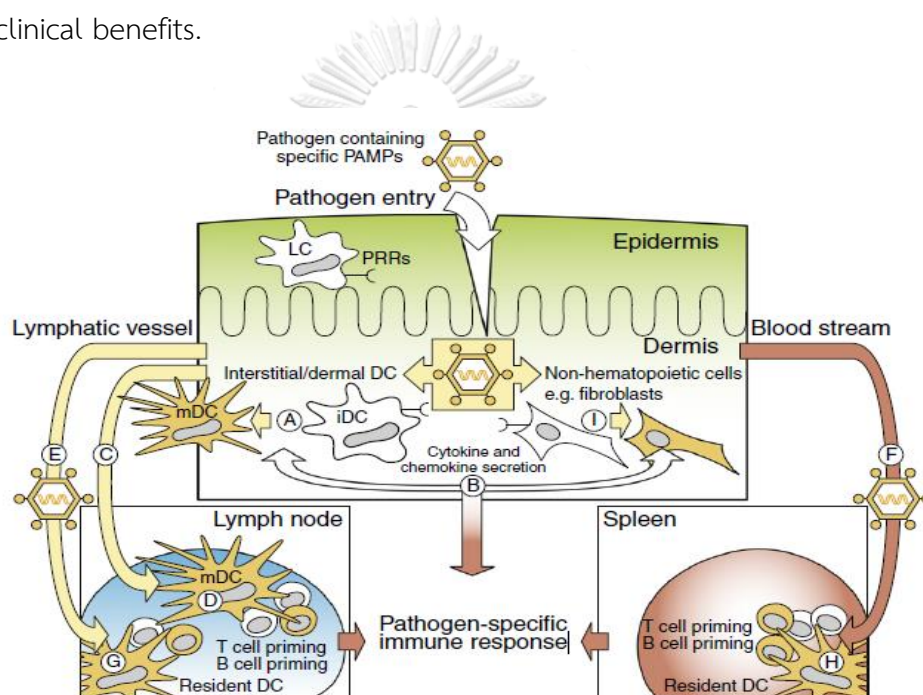


Figure 1 : Scheme of the activation of the immune system against pathogen after PAMP-PRR interaction from the pathogen entry into the cell. iDCs, interstitial dendritic cells; LC, Langerhans cells; mDC, mature DCs. (2)

2. Poly(I:C) as an immunostimulatory adjuvant

2.1 Signaling induced by poly(I:C)

One of the FDA approved potential immunostimulatory adjuvant candidate for novel vaccines is the synthetic double-stranded RNA (dsRNA), polyinosinic:polycytidylic

acid, normally denoted as poly(I:C) that comprising of two-annealed strands of different polymers includes inosine poly(I) strand and cytidine poly(C) strand, as shown in figure 2. A synthetic adjuvant is being used in clinical studies for infectious diseases and cancers. Since its structure mimics the viral dsRNA, It has been recognized as an potent Toll-like receptor 3 (TLR3) activator. TLR3 is a transmembrane protein sited on endosomal of antigen-presenting cells (APCs) and also many types of tumor cells. Moreover, another signaling pathway is also dependent on cytosolic melanoma differentiation-associated gene-5 (MDA-5) and cytosolic retinoic acid-inducible gene I (RIG-I) (7). Both endosomal and cytosolic sensors can encourage the productions of the strongest type I interferons and also inflammatory cytokines associated with innate and adaptive immunity (8, 9). Owing to poly(I:C) is PAMPs by self, thereby they tend to the antitumor responses and act through those specific immune-stimulatory mechanisms on APCs toward dendritic cell maturation, type I interferon production, and thus antigen-cross presentation to CD8+ T cells associated with adaptive immunity, and contribute to suboptimal induction of the cellular-mediated immune responses directly into the cancer microenvironments (9). Therefore, poly(I:C) has been promising well-defined adjuvant for the development of cancer immunotherapy.

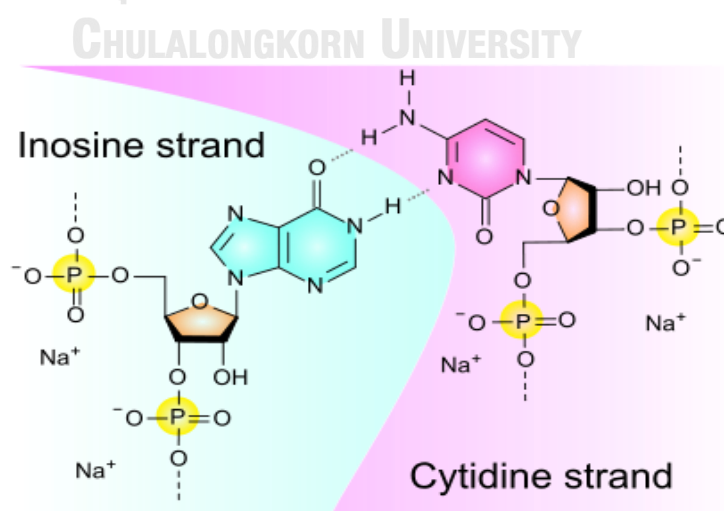


Figure 2 : Illustration of the poly(I:C) structure.

2.2 The major challenges of poly(I:C) in clinical trials

Since the synthetic dsRNA induced immune response is reported, the TLR3 ligand poly(I:C) has been spotlighted as an adjuvant on the field of cancer immunotherapy. Indeed, therapeutic cancers using poly(I:C) in clinical studies demonstrated the failure to present a favorable results of poly(I:C) (8). However, the soluble poly(I:C) possessed some concerns with low efficiency regarding the use in clinic. The molecule is inherently susceptible to rapid enzymatic degradation by RNase in tissues and serum, resulting in a short half-life in human plasma (<6 min) (3) as well as rapidly cleared after systemic injection. Moreover, there are many evidences for dose-dependent toxicity after administration of the adjuvant (3, 10). These drawbacks of poly(I:C) make the its limitations as used in clinical trials.

2.3 Derivative poly(I:C) in clinical study

Currently, besides an immunostimulant poly(I:C) that is widely used in clinical trials, another strong antiviral adjuvant, poly(ICLC), was designed as an advanced poly(I:C) analog. Poly(ICLC) was developed from complexation of the parent molecule with poly-L-lysine carboxymethyl cellulose. The analog was TLR3 agonist causing innate immune stimulation. It is mostly co-administered with the other immunostimulant vaccines for the maximized therapeutic effects to improve the clinical outcome by delaying the molecular degradation of the original form (11). However, the of poly(ICLC) efficiency remained similar to poly(I:C) with the comparably low level of cytokine production being elevated (12).

3. Overcoming poly(I:C) limitations by designing the particulate systems

Currently, the major focus in improving bioavailability and stability of the TLR3 agonist, poly(I:C), as a therapeutic vaccine adjuvant includes designing its carrier systems (2). Efficient delivery systems for cancer vaccines are needed to address its

instability and systemic toxicity limitations, as well as the enhancement of its property as adjuvanticity by targeting APCs. Various colloidal particulate systems (2, 13-15) have been investigated as carriers for the nucleic acid delivery in order to protect them from enzymatic degradation, elevate their bioavailability, and target the cell or tissue. The expectation lies on promising results in the improvement of the adjuvant activities, which could lead to administered dose reduction and absence in systemic side effects. As a matter of fact, the incorporation of adjuvant and carrier systems are being studied in both non-clinical and clinical trials (16).

4. Nanocarriers as ligand delivery

Nowadays, the progressive nanotechnology that suggested the nano-delivery system for particular formulations of ligands as an adjuvant in order to suitable delivery and reduce systemic side effects (16, 17). Many advantages of the incorporation of the immunostimulatory ligands with suitable nano-delivery systems affect the vaccine efficiency which recent efforts to make safe and efficient vaccine. The delivery of the potential ligands to APCs directly can reduce the administered dose and needless side effects of adjuvants/ligands. Moreover, the sustained immune stimulation can be obtained by localized depot of the ligands to desire tissues (such as, immune cells and lymphoid tissues) for the immuno-stimulation effects along with the potential CTLs responses against cancer cells. Among the nanoparticle vaccinations indicated immune efficacy of the load both adjuvant and antigens delivery into the target DCs enabling capture, process and cross-presentation to CD8+ cytotoxic T lymphocytes. In point of fact, the incorporation of adjuvant and carrier systems are studied in non-clinical and clinical trials. Especially, It has been suggested that more efficient of the cross-presentation when co-delivered with a danger signal. Moreover, the polyvalent ligands can be design by particulate nanogels, which can encourage the cluster of

receptor-mediated endocytosis on targeted immune cells, and then potential immuno-stimulation.

5. Nanogels

5.1 Nanogels-based delivery systems

In recent years, the novel innovation of nanotechnology has been progressing in the field of drug delivery. Among many types of sub-micron particulate drug carriers, the outstanding hydrophilic nanogel-based, non-viral vectors are the systems of interest (18). Nanogels is a kind of the macromolecular hydrogels that polymer networks are physical/chemical crosslinked within the three dimensional size of sub-micron particles. Nanogels can formed by covalent bonding or self-assembly (non-covalent bond) methods. There are many types of nanogels; nanogels classified by the kind of polymer crosslinkers including physical/chemical crosslinks; nanogels categorized by the bond between drug and polymer, e.g. physical encapsulations (vanderwaal, hydrogen bond and hydrophobic interaction) and chemical/bio conjugations; the classification of nanogels based on preparation techniques; nanogels can be also categorized by the types of polymer used including synthetic and natural polymers (19).

5.2 Advantages of nanogels

Nanogel represent candidates of drug carrier systems for different types of therapeutic molecules in the field of cancer immunotherapy. Firstly, nanogels can provide special features from their physicochemical properties, compared to other traditional drug delivery systems (20). Secondly, the nanoscale-sized hydrogels with three-dimensional network structures provide a high water-content property and high biocompatibility that leads to the stability of the colloidal system avoiding particle

aggregation in the bloodstream (21). Thirdly, the tunable polymeric network can be used to incorporate different types of therapeutic molecules including drugs, nucleic acids and proteins (22). As a result, the payload can be protected from both enzymatic/chemical degradation with the extended the circulation time of the incorporated components (23). In contrast to the conventional hydrogel or macrogel, the nano-sized hydrogels can be administered through intravenous injection giving the benefit of improved biodistribution. More importantly, hydrophilic nanogels are used to control release of the delivered therapeutic agents by incorporating within polymer networks.

The controlled release of loaded therapeutic agents is a pivotal role in successful drug delivery. First, to avoid the unneeded adverse effects from a highly administered dose, the drug or payload should be available at the target site in therapeutic concentration. Second, the high surface area of hydrophilic nano-sized hydrogels is more beneficial in the transient controlling drug release rates than micro-sized systems. Finally, the release profile can affect cellular uptake, the nanogel as a whole were internalized into cells via endocytosis and introduce its way towards the intracellular target region, leading to the significant enhancement of the therapeutic effects (24).

5.3 Nanogels for the poly(I:C) delivery

The nano-sized hydrogels based cancer vaccine delivery system show promise as a proper platform for improve the efficiency of adjuvants for cancer immunotherapy, owing to they have provided available for multiple advantages by additional characterization into the loaded molecules, as such nanogels can enhance these properties including solubility, bioavailability, stability and safety. The particulate of poly(I:C) can be achieved by several types of loading, including physical/chemical approaches. However, the development should be considered to the targeted APCs in

order to further activation of the potential cytotoxic T cell responses through cross-presentation on co-stimulatory molecules of MHC class I (25).

For example, the development of cancer vaccine delivery based on nanogel systems for targeted and controlled release approaches had good potential in animal vaccination studies. The positive charges of dextran nanogel (size around 200 nm in diameter) achieved by reducible disulfide-conjugating with ovalbumin (OVA) as an antigen model and combining with the potential adjuvant, poly(I:C), which can evoke the danger signal through TLR3 pathway. This system shows efficiently taken up and activated the dendritic cell maturation *in vitro*, further the antigens were processed when delivery into the cytosol via reducing bonds with redox-sensitive and induced robust antigen specific T cell responses. Moreover, thereby induced a strong prophylactic and therapeutic effect against tumor in mouse model (26).

As shown in figure 3, a cationic chitosan nanoparticle-based cancer vaccines (27) had been promising nanoparticle platforms for intracellular delivery of adjuvant and antigen to endosomal TLR3 by DCs targeting to induce specific CD8⁺ T cell against their tumors and enhanced tumor therapeutic efficacy. The nanoparticle co-encapsulating an antigen (OVA) and influence adjuvant, poly(I:C), by ionic interaction, with a mean diameter of approximately 250 nm and showed the potential in *in vivo* intracellular delivery into DCs contributed to DC maturation and stimulation of cytotoxic CD8⁺ T cells through cross-presentation of antigens in tumor-bearing mice (17).

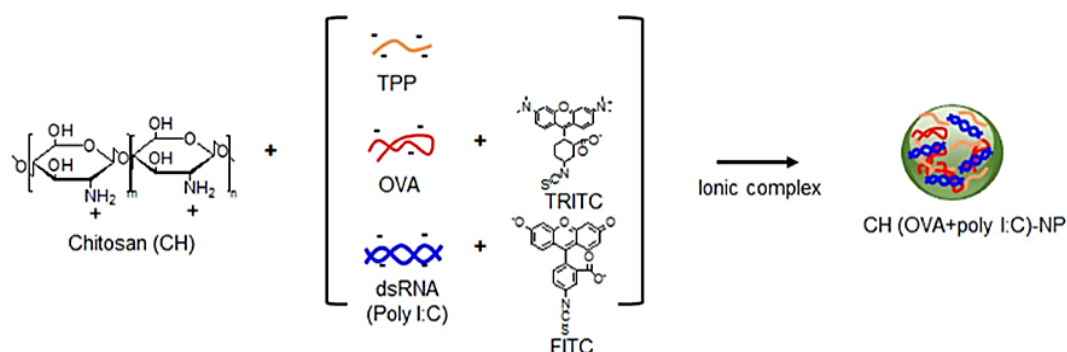


Figure 3 : Schematic of chitosan nanoparticles encapsulating an adjuvant and OVA as an antigen model, and the nanoparticle prepared by ionic complex (27).

6. Hyaluronic acid

Hyaluronic acid (HA) or hyaluronan is a naturally occurring polysaccharide that is mostly present in biological fluids and tissues, especially as a main component of the extracellular matrix and an important molecule for maintenance of cartilage structure (28). Hyaluronan has a diverse biological activity from its properties as composed of a connective tissue microenvironment, including for cell survival, proliferation, and differentiation. HA is available commercially in a wide range of many forms that can be synthesized by the variety of cells, such as fibroblasts (29). Several research reports indicated that hyaluronic acid-based nanogels have been attractive as a biomaterial used for the development of drug delivery systems. The beneficial properties of these materials over other delivery platforms that are being studied for human clinical trials included 1) the extremely hydrophilic structure of the backbone with high water absorption making them safe for bioorganisms; 2) biodegradability; 3) simplicity for bioconjugation; 4) non-immunogenicity; and 5) high drug loading capacity from the porous polymer networks.

The linear HA formed from a repeating disaccharide units containing N-acetyl-D-glucosamine and D-glucuronic acid with interglycosidic linkages (figure 4). Actually,

HA is a negatively charged polymer associated with pH values from the carboxyl group of D-glucuronic acid, and forms of sodium hyaluronate in physiological conditions. It is possible to modify HA on the three available principle sites on HA structure, including hydroxyl and carboxylic group, as well as the N-acetyl group that allows HA functionalization (30). HA conjugation, inclusive of the polymer grafting usually occurs on the amide bonding within the N-acetyl group to link amine to the carboxyl group. The Carboxyl group can be activated using EDC/NHS coupling reaction for amide formation, which is a standard approach for bioconjugations.

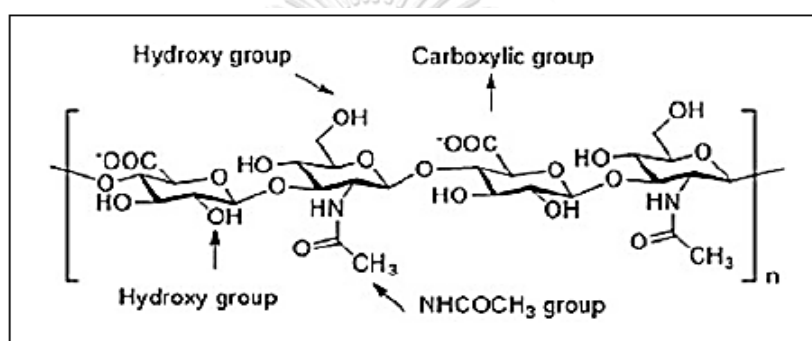


Figure 4 : Illustration of the structure of hyaluronic acid consisting of disaccharide repeating units and the main functional groups for chemical modification (31).

6.1 Hyaluronic acid targeting to CD44 receptor

Furthermore, HA has a capacity of selective internalization via specific cells that express of the CD44 receptor or HA-binding protein (32), which are presented in many kinds of cancer cells or immune cells (33-35). After the internalization of HA, it would be hydrolyzed by hyaluronidase inside the cells (36). Therefore, CD44 receptor have been choosing as a main tool for targeting of HA in many biomedical applications. To this end, the excellent properties of hyaluronan have significantly encouraged research in developing nano delivery systems that actively target drugs and genes against desirable cells, while reducing the toxicity.

6.2 Nanogel based on hyaluronic acid

A natural polysaccharide-based biocompatible nanogels have shown good potential for many biomedical applications. The several of researches reported hyaluronic acid-based nanogels have been interesting as the development in drug delivery. Due to many advantages appropriately of HA nanogels for human clinical trials over the other platforms: the ability of biocompatibility from the water absorption of backbone composing of hydrophilic residues, cause HA are safe for bioorganisms; biodegradability; simplicity for bioconjugation; non-immunogenicity; and high drug loading capacity from the porous polymer networks.

Consequently, HA-based colloiddally biocompatible nanogels have been extensively employed for the drug/gene delivery. Indeed, T. Fernandes Stefanello and his team (37) indicated that their biocompatible HA based on nanogels modified with the temperature-sensitive copolymers of ethylene glycol methacrylate (DEGMA and OEGMA) onto HA derivative backbone prepared by radical coupling reaction can successfully improve both *in vitro* and *in vivo* efficacy of the hydrophobic modeling drug by targeting to directly phagocytic murine macrophages through CD44 receptor-mediated endocytosis, while remains the safety. Furthermore, the drug-conjugated HA nanogels (20-40 nm) of Wei X. *et al.* can excellently improve the bioavailability of low-soluble anticancer drugs *in vitro* in drug-resistant human breast and pancreatic adenocarcinoma cells (38). Recently, the delivery of macromolecules i.e. nucleic acids by utilizing HA-based nanogels have been developed, because such nucleotides mostly undergo instability from enzymatic degradation in the serum or body fluids. For instance, thiol groups can be linked to thiol-HA conjugates with disulfide bonds to form the degradable HA nanogels in diameter ranging from 200 – 500 nm through the water-in-oil emulsion process. These nanogels were physically encapsulated with small interfering (siRNA) that is a rapidly degraded dsRNA in treating cancer, and their release

profile was dependent on amounts of the intracellular reductive molecules and further can uptake into the CD44-overexpressed cells (39).

7. Poly (N-isopropylacrylamide)

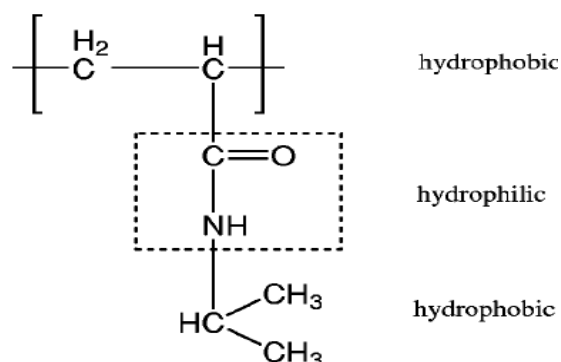


Figure 5 : The structure of poly(N-isopropylacrylamide) (pNIPAM) (40).

Poly(N-isopropylacrylamide) or pNIPAM is one of the most well-known thermal sensitive polymer that made up from hydrophobic (isopropyl group) and hydrophilic (amide group) residues (figure 5), as it undergoes reversible phase transition when the temperature above its lower critical solution temperature (LCST) resulting in the conformational and property alterations (41, 42). In this regard, pNIPAM exhibits a lower critical solution temperature (LCST) of 32 °C, which is a large benefit in many biomedical applications, in particular for drug delivery systems, because it is close to the temperature of the human body (43). When temperatures above its LCST, they are collapsed and expose turbidity as a cloud point in the water, due to the hydrophobic effects from the hydrogen bonds interacting between water molecules and hydrophilic segments are disrupted. This causes polymer-intrapolymer interactions of hydrophobic moieties on polymeric chains, driving the polymer aggregation and phase transition occurs (41, 42). For this reason, the LCST of this polymer has been utilized as an intelligently thermoresponsive polymer to create a dramatic switch on-off delivery platform in the controlling of targeted drug release (44, 45). The LCST of pNIPAM can be tunable to the appropriate application used by copolymerizing with a hydrophobic

polymer to LCST decreasing or elevating the LCST behaviors through the addition of hydrophilic polymers. In one of the studies, a copolymerization of pNIPAM with methacrylic acid and the hydrophilic polyethylene glycol (PEG) increased the LCST from 32°C to 38°C, resulting in the pH-thermal responsive polymer for utilizing in drug delivery (46).

Development of a stimuli-responsive nanogel delivery system has plenty of attention in recent years since these systems can drive assembly as well as a sol-gel phase transition of composite polymers induced by surrounding environments such as pH, temperatures, ions and convert of specific molecules. These stimuli-responsive nanogels present exclusive advantages toward drug carriers, including the tunable size in nano- to microscale, various types of drug payloads, high surface areas and drug loading capacity, targeted delivery property by specific functionalization, and controllable drug release. Indeed, the conjugation of pNIPAM-based thermal sensitive polymers with natural biodegradable and biocompatible polysaccharides such as chitosan, dextran and hyaluronan have been carried out in various studies to fabricate the self-aggregated nanoscale of hydrogels as promising candidates for the delivery of bioactive molecules including cancer therapeutics. In this regard, in vitro studies has been recently reported that thermosensitive pNIPAM segment grafted onto chitosan polymeric backbone as a thermal-induced self-assembled nanogels, such system can improve the bioavailability of hydrophobic drug curcumin, control of the drug release rate from the porous structure of polymer networks as display a smart thermoresponsive polymer, and enhanced signification of anti-cancer activity (47). In another one of studies reported that the thermal motivated nanogel synthesized from pNIPAM conjugating with HA as a skeletal structure by using disulfide linker, these systems allowed the glutathione-triggered doxorubicin release from polymer networks into A549 lung cancer cell, and exhibited safety and enhanced the potential of antitumor activity towards in vivo tumor-bearing mice (48).

CHAPTER III

METHODOLOGY

Chemicals and materials

Sodium hyaluronate (MW 47 kDa) was purchased from Liuzhou Shengqiang Biotech Co., Ltd, China, poly-(N-isopropylacrylamide) (pNIPAM; MW 5.5 kDa) and N-hydroxysuccinimide (NHS) were obtained Sigma-Aldrich, USA. 1-ethyl-3-(3-dimethylaminopropyl) carbodiimide hydrochloride (EDC) was purchased from CreoSalus Inc., USA. Deuterium oxide was purchased from Cambridge Isotope Laboratories, Inc., USA. As a ligand for TLR3, polyinosine-polycytidylic acid (poly(I:C)) high molecular weight (1 mg/mL in PBS) was obtained from faculty of medicine, Chulalongkorn university and Rhodamine-labeled poly(I:C) was purchased from *Invivogen*, USA. The RAW 264.7 murine macrophage cell lines was obtained from Chawanphat Muangnoi, Ph.D. (Cell and Animal Model Unit, Institute of Nutrition, Mahidol University). Fetal bovine serum (FBS), L-glutamine (200 mM), ActinGreen™, and DAPI were acquired from Sigma. A PrestoBlue™ cell viability reagent was obtained from *Invitrogen*. Dulbecco's modified Eagle's medium (DMEM) and penicillin-streptomycin were purchased from *Invitrogen*. Hyaluronidase from bovine testis was obtained from Sigma Aldrich (ref. H3506, 451 Units/mg).

Methods

1. Synthesis of pNIPAM grafted hyaluronic acid.

The nanogel was prepared by self-assembling of amine-terminated pNIPAM (pNIPAM-NH₂) grafted onto hyaluronic acid (HA) backbone in 5% degree of modification were synthesized by using an EDC/NHS peptide coupling reaction for amide

conjugation as reported previously (49). The mole of pNIPAM-NH₂ was calculated via an equation:

$$\text{Degree of modification (\%)} = (\text{mole of pNIPAM-NH}_2 / \text{mole of HA monomer}) \times 100$$

Briefly, 47×10^3 g/mol of HA sodium salt was dissolved in 25 mL ultrapure water at 0.5% w/v (0.5 g, 1.26 mmol of COOH). The amounts of amine-terminated pNIPAM with M_n equal to 5.5×10^3 g/mol was added at 1:0.05 of HA:pNIPAM molar ratio (0.3465 g, 0.063 mmol of NH₂) for grafted HA backbone in 25 mL ultrapure water. Next, EDC/NHS was then added in powder to HA-pNIPAM solution by 1:4:4 molar ratio of HA to EDC and NHS coupling chemical (0.966 g EDC and 0.58 g NHS), to activated pNIPAM-NH₂ and HA polymers at room temperature (around 27 °C). The pH was adjusted to 5.5 ± 0.3 (using 5M HCl and 5M NaOH solutions). After an hour, pH was settled at 7.5 ± 0.3 . The conjugating reaction was allowed for 48 hrs at room temperature under constant stirring before purifying by dialyzing (A dialysis membrane: MWCO 10500) against ultrapure water for 3 days to remove unreacted synthesis parent compounds following by the lyophilization 3 days (Labconco Lyophilizer). The lyophilied polymer was stored at -20 °C.

¹H NMR was carried out to confirm the resulting products. The synthesized polymer was named HA-g-pNI. The samples in D₂O were used for ¹H NMR spectra and confirm the conjugation of pNIPAM to HA backbone from the integration ratio between their characteristic peaks.

2. Preparation of HA-g-pNI nanogel and nucleic acid loading.

To prepare poly(I:C) incorporating HA-g-pNI nanogels, gel was prepared by a simple sonication method in aqueous conditions using 0.1, 0.25, and 0.5 (% w/v) of HA-g-pNI polymer in sterile ultrapure water. After sonication for 30 minutes at room temperature, the nanogels was settled for overnight at 4 °C and then centrifugation at

25 °C for 5 minutes at 3000 g. An incubation method was performed for the HA-g-pNI nanogel loaded with poly(I:C). In brief, 100 µL of poly(I:C) in concentrations of 0.2, 1, and 10 µg/mL were then added dropwise to 1 mL of each HA-g-pNI solutions. The poly(I:C) incorporated nanogels spontaneously formed with constant stirring (250 rpm, 30 min) at 25 °C, leading to poly(I:C)-loaded HA-g-pNI nanogels. The prepared nanogels were stored at 4 °C and used in each experiment as prepared freshly.

3. Characterization of adjuvant-free and poly(I:C) nanogels

All of the nanogel formulations were characterized by dynamic light scattering (DLS; Zetasizer NanoZS, Malvern instruments Ltd.) for their particle size, size distribution, and net surface charge (zeta-potential). Transmission electron microscopy (TEM) was observed for their morphology. The lower critical solution temperature (LCST) was investigated as the temperature that causes particle size changes instantly. The controlled temperature program is increased from 25 to 40 °C at 1 °C/min in each sample solution. All measurements were made in triplicate and data are reported as a mean ± standard deviation.

4. Formation of poly(I:C)-incorporated HA-g-pNI nanogels.

To determine that the incorporation of poly(I:C) remained intact within the HA-g-pNIPAM assembly, a hyaluronidase was used to facilitate the poly(I:C) release from the assembled nanogels by hydrolyzing the HA polymeric chain into the oligo hyaluronan. All of the poly(I:C) nanogel formulations (0.1 mL) was incubated with 200 U of hyaluronidase in an mM buffer for 4 hrs at 37 °C before analyzing with gel electrophoresis. Briefly, 0.02 mL of each poly(I:C)-loaded nanogel formulations was loaded in the well of 1% (w/v) agarose gel containing Visafe Green (1:10,000) at 0.2, 1 and 10 µg/mL of poly(I:C) concentrations. After applying 110 V electrodes in TAE buffer (50mM Trisma-base, 20mM glacial acetic acid, 1mM EDTA, pH 8.0) for 20 minutes, the

gel was analyzed with blue light. The positive and negative controls are the equal poly(I:C) amounts and the naked HA-g-pNI nanogels, respectively.

5. *In vitro* physiological stability of poly(I:C) within nanogels

Nuclease protection assay was performed to indicate the serum protection of the HA-g-pNI nanogel system. For the poly(I:C) nanogel stability test, various amounts of HA-g-pNI nanogels (0.1, 0.25 and 0.5 % w/v) loaded with poly(I:C) and poly(I:C) in solution at a concentration of 10 µg/mL of poly(I:C) were immersed in medium containing 95% fetal bovine serum (FBS) and continue to incubation at 37 °C for 1, 3, 6 and 24 hrs. At different time intervals, 200 µL suspension was withdrawn to analyze the degraded RNA by a gel electrophoresis (described above), and the degraded poly(I:C) was visualized with the blue light. The degradation of poly(I:C) can be detected by the significant increase of its higher intensity than the band of the non-treated poly(I:C) nanogel. A positive control was the equal amounts of poly(I:C) solutions.

6. Cell viability assay

The PrestoBlue® cell viability assay was performed for determining the cytotoxicity of all formulation. RAW 264.7 macrophage cell lines will be maintained in DMEM supplemented with 10% (v/v) FBS containing 1% penicillin-streptomycin. 5×10^4 cells/well were seeded on 96-well plates and incubated in 5% CO₂ atmosphere incubator at 37 °C. After 24 hrs, the medium was replaced with fresh serum-free medium and the cells were treated with all poly(I:C) nanogel formulations and its soluble (equivalent poly(I:C) concentration: 0.2, 1, and 10 µg/mL, respectively). The next day, the cell was incubated with 100 µL of 1 µg/mL PrestoBlue solution, for 1 h at 37 °C. The PrestoBlue solution without cells was used as a blank for normal condition and cell plus medium only was used as a positive controls. All experiments

were carried out in triplicate. Lastly, the purple PrestoBlue absorbance was measured as the living cells using a microplate reader (CALIOstar) with the wavelength at 590 nm. The viability of the cells was calculated from the optical density (OD) values of each treatment according to the following equation.

$$\% \text{ Cell viability} = (\text{OD}_{\text{treated cells}} - \text{OD}_{\text{blank}} / \text{OD}_{\text{positive control}} - \text{OD}_{\text{blank}}) \times 100$$

7. *In vitro* cellular uptake study of poly(I:C)

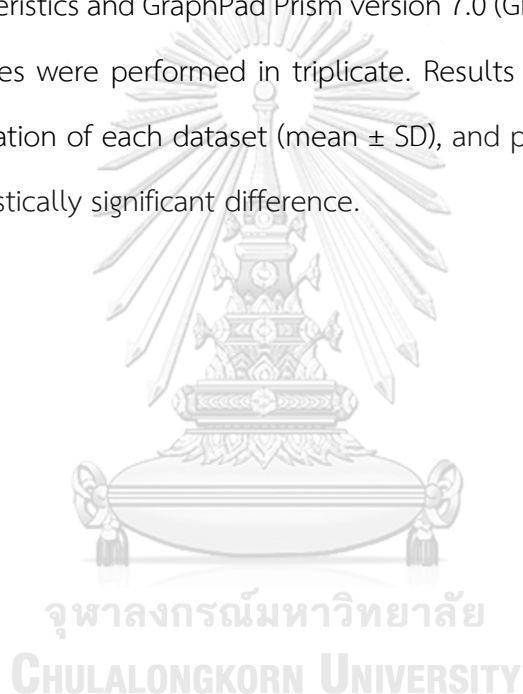
To assess the internalization of poly(I:C) entrapping in the HA-based nanogels into the antigen-presenting cells, RAW 264.7 murine macrophage cell lines was used as a representative of this cell. Qualitative fluorescence microscopy was performed using a rhodamine-labeled poly(I:C) for poly(I:C) visualization.

We would be verified as to what poly(I:C) encapsulation by HA-g-pNI nanogels improves its uptake by macrophages rather than its soluble. Cells was incubated with 1 $\mu\text{g}/\text{mL}$ rhodamine-tagged poly(I:C) nanogels or rhodamine-tagged poly(I:C) solution. Briefly, RAW 264.7 murine macrophage cell lines was cultured in 96-well culture plates in a seeding density of 5×10^4 cells per well with culture medium supplemented with 10% (v/v) fetal bovine serum (FBS), 1% penicillin-streptomycin. After 24 hrs incubation to allow the cell adherence at 37°C in a 5% humidified CO₂ atmosphere, the culture medium was removed and then cells was once washed with basal medium (DMEM), followed by adding 150 μL serum-free medium containing rhodamine-labeled poly(I:C) nanogels or soluble poly(I:C)-rhodamine at 1 $\mu\text{g}/\text{mL}$ of poly(I:C)-rhodamine concentration. After 24 hrs incubation, the cells was washed once with basal medium to remove unbound nanoparticles and fixed with 4% (w/v) paraformaldehyde in PBS for 15 min, following by once PBS wash and subjected to nuclei staining by DAPI for 30 min and then stained with ActinGreen™ 488 for 30 minutes to cell structure marker. Fluorescence microscopy was carried out to examine cellular internalization of all

poly(I:C) loaded HA-g-pNI nanogel formulations. Negative control consists of naïve cells and culture medium only. The resulting fluorescence emissions were acquired using 546-576 nm (for poly(I:C)-rhodamine), 425-475 nm (for DAPI), and 515-565 nm (for ActinGreen™ 488).

8. Statistical analysis

Statistical analysis was carried out using IBM SPSS Statistics 23 with one-way ANOVA for characteristics and GraphPad Prism version 7.0 (GraphPad Inc.) for expressing the data. All studies were performed in triplicate. Results were indicated as a mean and standard deviation of each dataset (mean \pm SD), and p values of 0.05 or less was accepted the statistically significant difference.



CHAPTER IV

RESULTS AND DISCUSSIONS

I. Synthesis and characterization of pNIPAM grafted HA

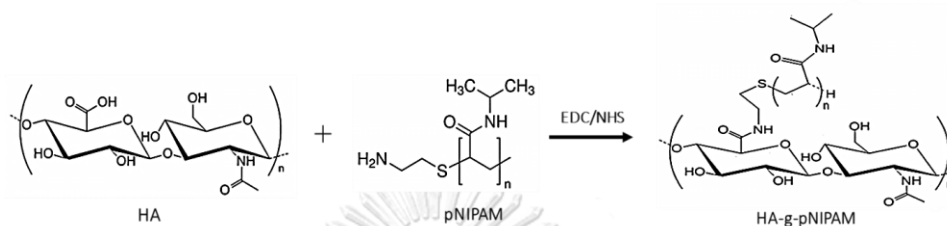


Figure 6 : Schematic illustration of the procedures for the synthesis of pNIPAM grafting polymer on HA as a backbone through EDC/NHS coupling reaction (50, 51).

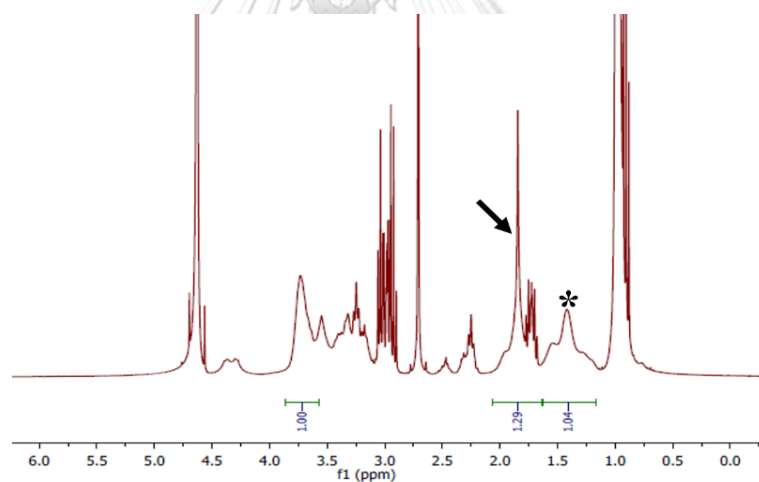


Figure 7 : ^1H NMR spectra of pNIPAM-grafted hyaluronic acid (HA-g-pNI) with 4% degrees of modification. Arrowed peak indicates the protons that interfere between a proton on a chiral carbon of pNIPAM chain and protons belong to the N-acetyl group of HA backbone. Asterisk peak represents the H_2 protons on C1 at the attached pNIPAM chain.

To achieve an effective nucleic acid delivery of the nanocarrier, HA-pNIPAM (can be abbreviated here as HA-g-pNI) grafted copolymer was prepared as previously

reported (50, 51). EDC/NHS coupling reaction was used to coupling pNIPAM to hyaluronic acid by amide conjugation, as shown in figure 6. The structure of each conjugating reaction product in polymer synthesis was confirmed via ^1H NMR spectra (see figure 7). The HNMR spectra of pNIPAM-grafted HA could exhibit the successful grafting of pNIPAM. The pNIPAM-grafted HA was produced with degree of substitution of approximately 4%.

II. Physical characterization of adjuvant-free nanogels

Here, we fabricated the self-assembled HA-g-pNI nanogels by subsequent sonication of the grafted polymer to obtain the nanogel particle formulation. Three different polymer concentrations were used to form the nanogel formulations in water at 0.1, 0.25, and 0.5 (% w/v) of the HA-g-pNI polymer. Characterization for the mean size, PDI, and zeta-potential were investigated by DLS to observed physical properties in each of the formulations.

In this study, we indicated that the concentration of polymer (% w/v) has direct effect to the diameter size of nanogel particle. We found that the particle size of the nanogels increased as the concentration increased (the data was indicated as mean \pm standard deviations; table 1). The DLS results showed the fine controlled of particle size of blank nanogels within approximately 700-900 nm of diameter range (see figure 8b). The sizing indicated the different signification in statistical analysis comparing between the nanogel formulations with the grafted polymer at 0.1 and 0.5 (% w/v), and at 0.25 and 0.5 (% w/v). However, the mean particle size difference was not signification, statistically, when comparing nanogel formulations with 0.1 and 0.25 (% w/v) of polymer. The size distribution of nanogel solution was determined as the PDI values. The nanogel solutions showed PDI values of approximately 0.37-0.66, indicating these formulations are quite polydispersed as the characteristic of swellable nanogel

(see figure 8b and table 1). The zeta-potential of the HA-g-pNI nanogel formulations displayed small negative charge repulsion in the water of approximately -17 to -26 mV. This probably caused by the remaining carboxylic group on HA parent chain. The small variations in zeta-potential among each formulation was not statistically significant (see figure 8b and table 1).



Table 1 : Research plan 1 Physical properties of the HA-g-pNI nanogels and the poly(I:C) loaded nanogels in each formulation measured by DLS.

Nanogel formulations	Z-average (d.nm)	PDI	Zeta-potential (mV)
<i>I. Blank nanogels</i>			
0.1% HA-g-pNI	699 ± 45.97	0.39 ± 0.035	-26.5 ± 5.74
0.25% HA-g-pNI	754.8 ± 14.71	0.66 ± 0.521	-24.6 ± 3.13
0.5% HA-g-pNI	941.8 ± 69.88	0.37 ± 0.316	-17.5 ± 0.75
<i>II. Nanogels (% w/v) + poly(I:C) (µg/mL).</i>			
0.1% + 0.2	389.3 ± 92.71	0.46 ± 0.032	-22 ± 1.7
0.1% + 1	369.1 ± 98.71	0.48 ± 0.047	-14 ± 10.9
0.1% + 10	627.3 ± 92.53	0.56 ± 0.121	-20 ± 6.5
0.25% + 0.2	1095 ± 688.54	0.68 ± 0.226	-23 ± 6.1
0.25% + 1	303.9 ± 289.65	0.86 ± 0.234	-20 ± 6.1
0.25% + 10	493.9 ± 273.54	0.72 ± 0.224	-20 ± 7.6
0.5% + 0.2	313 ± 45.27	0.87 ± 0.148	-23 ± 4.8
0.5% + 1	578 ± 49.75	0.63 ± 0.134	-21 ± 5.0
0.5% + 10	1034.9 ± 88.26	0.59 ± 0.132	-23 ± 5.0
<i>III. Nanogels (% w/v) + poly(I:C) (µg/mL): upon incubation continuously.</i>			
0.1% + 0.2	103.2 ± 2.65	0.52 ± 0.525	-19 ± 1.2
0.1% + 1	172 ± 2.41	0.37 ± 0.101	-22 ± 2.4
0.1% + 10	126.8 ± 2.58	0.38 ± 0.105	-21 ± 2.9
0.25% + 0.2	116.6 ± 1.80	0.48 ± 0.004	-25 ± 5.1
0.25% + 1	155.2 ± 5.88	0.50 ± 0.013	-24 ± 5.1
0.25% + 10	322.3 ± 28.12	0.45 ± 0.088	-20 ± 5.0
0.5% + 0.2	310.4 ± 10.10	0.38 ± 0.132	-22 ± 3.6
0.5% + 1	556.4 ± 88.87	0.55 ± 0.401	-21 ± 5.0
0.5% + 10	1,077.3 ± 143.46	0.47 ± 0.396	-24 ± 3.0

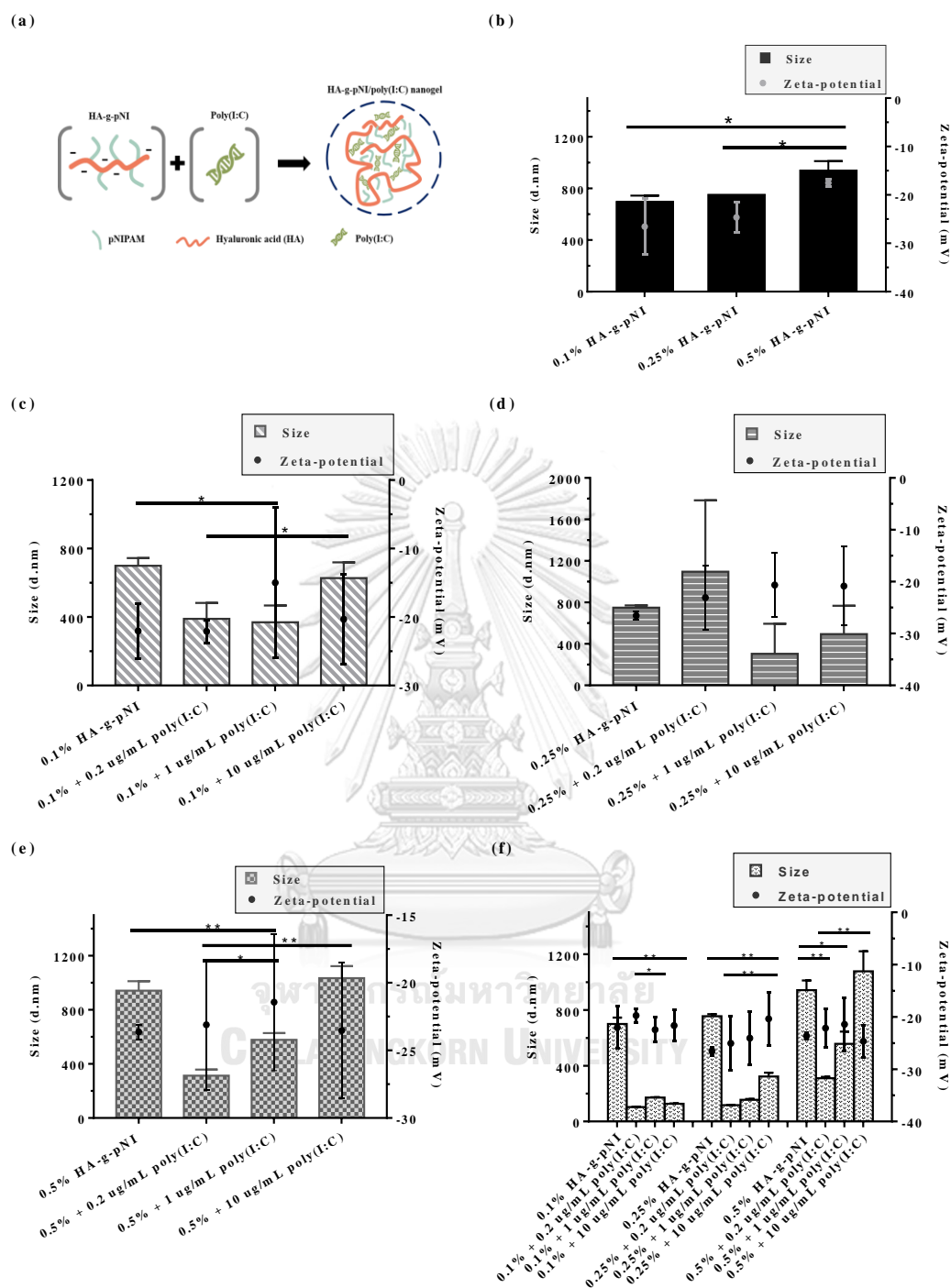


Figure 8 : Physical properties of HA-g-pNI nanogels and adjuvant-loaded HA-g-pNI nanogels. The mean size and zeta-potential value of the nanogel particles measured by DLS. (a) Schematic representation of poly(I:C)-loaded HA-g-pNI nanogels prepared by physical incorporation. (b) Size and surface charge of the blank HA-g-pNI nanogels.

*Comparison between the mean size and surface charge of the blank nanogels and loaded nanogels within each of polymer ratios, including (c) 0.1, (d) 0.25, and (e) 0.5 (%w/v). (f) Size and surface charge of each nanogel formulation when continuous incubation (for 10 days) at 4 °C. The signification were indicated as * $p < 0.05$ and ** $p < 0.001$.*

III. Preparation and characterization of the adjuvant-loaded hyaluronic acid nanogels

Biodegradable nanogels, particularly hyaluronic acid (HA) based nanogel formulations have attracted significant attention as nanomaterials for the design of biotherapeutic delivery carriers (52). In this study, we successfully fabricated the HA-grafted pNIPAM nanogel carriers, with encapsulation of an TLR3 immunostimulatory adjuvant, poly(I:C) within HA-g-pNI nanogel network (figure 8a). The association of the adjuvant and polymeric assembly was based on a simple entrapment method via physical interaction between polymers and the adjuvant.

The HA-g-pNI nanogels were prepared by grafting pNIPAM onto HA, further sonication method for obtaining the self-assembled nanogel particle, and introduction of poly(I:C). 0.1, 0.25 and 0.5 (% w/v) of each polymer in ultrapure water were carried out to form nanogels formulations by incubation with each of poly(I:C) concentrations. The physical properties of the adjuvant loaded nanogels were characterized by DLS measurement at the time of incubation.

The nucleic acid–polymer ratio enabled control over nanogel size. We observed such effect when keeping the amount of HA-g-pNI constant with varied amount of the loaded adjuvant, as shown in figure 8c, 8e and table 1. At the 30 minutes of incubation, the formulations with 0.1% (w/v) HA-g-pNI loaded with poly(I:C) at 0.2 and 1 $\mu\text{g/mL}$

resulted in smaller average diameter of the nanogels, with the sizes close to 400 nm with PDI around 0.4, comparing to their blank nanogel without poly(I:C).

No significant differences in average sizes (around 200-1,100 nm range; PDI: 0.6-0.7) per poly(I:C) concentration rise in the group of formulations containing 0.25% (w/v) HA-g-pNI at 30 minutes of incubation (see figure 8d and table 1). The mean particle size of each of 0.5% (w/v) HA-g-pNI formulations with poly(I:C) encapsulation had significant size difference in the range of 300-1,000 nm with the increasing concentration of poly(I:C) loads, while high PDI values varied in the range around 0.6-0.9 at 30 minutes of incubation (see figure 8e and table 1). The size of 0.5% (w/v) gel loaded with adjuvant concentrations at 0.2 and 1 $\mu\text{g}/\text{mL}$ reduced with significant differences (around 300-600 nm range; PDI: 0.6-0.8) when compared to the blank nanogel. All nanogels presented the negative charge with no significant differences in the range of -14 to -23 mV of the particle surface charges.

Moreover, we observed slight change in size distribution across all nanogel formulations with different incubation time. 0.1% (w/v) HA-g-pNI loaded with all adjuvant concentrations and 0.25% (w/v) HA-g-pNI loaded with 0.2 $\mu\text{g}/\text{mL}$ poly(I:C) had significantly decreased in the average size (by 100-170 nm) upon the continuous incubation for 10 days at 4 °C compared with day 0 measurement, as in shown figure 8f and table 1. In addition, we founded the significant difference in size of particles that loaded with all concentrations of poly(I:C) in 0.25% (w/v) HA-g-pNI, compared with blank HA-g-pNI nanogel. The study suggested that the longer incubation time could contribute to the smaller size and size distribution of the poly(I:C) nanogels in water. The decrease in size and PDI of the loaded particles after continuous incubation might be caused by the equilibrium state of poly(I:C)-polymer interactions. The happening of the decreased diameter size of the nanoparticles after poly(I:C) loading indicated that

the hydrophilic poly(I:C) had interacted with the hydrophilic HA chain in the assembly, causing the decrease of HA polymeric chain and also minimize of the nanogel particles.

In contrast, all concentrations of poly(I:C) incorporations with 0.5% (w/v) HA-g-pNI showed no differences in particle size alterations (around 400-1000 nm) per incubation time (figure 8e, 8f and table1). This could be the reason that polymer concentration affects the particle size and physical stability of the nanogel particles in corresponding with the other report previously (53).

No significant differences in the zeta-potential changes in all formulations (with- and without- poly(I:C) loads), accordingly. However, the particle size and surface charge had most effects upon immune cell association. The negatively charged nanoparticles can cause some degree of efficiently particle uptake on the immune cells such as an dendritic cells (4) as well as THP-1 macrophages (54). Therefore, our developed nanogel formulations maybe successful for the application in cell-based assay.

IV. Nanogel morphology

The morphology of the nanogel particles were indicated by TEM images, shown in figure 9. TEM images represented the HA-g-pNI nanoparticles formed with three different amounts of polymer in aqueous dispersion. They were almost spherical in shape with rough edge, possibly as the particles' swollen surface. Polydispersed size of around 200 nm to 1 μ m was demonstrated supporting the hydrodynamic sizing by DLS. The particles were well distributed due to the slight negatively charge on the nanoparticle surface. The nanoparticles formed with poly(I:C) showed even more irregularly spherical shape with higher degree of roughness in their surface nanostructures. Moreover, the size in diameter varied between 200-1,000 nm range, as illustrated in Figure 9A and 9C. For the figure 9b indicated the difference in the surface nanostructures between naked nanogel and poly(I:C)-loaded nanogels in formulations of 0.1% HA-g-pNI loaded with 1 and 10 μ g/mL poly(I:C). The loaded nanogels indicated

spherical in shape with more roughness of loaded particles. Moreover, 0.5% (w/v) HA-g-pNIPAM formulation loaded with poly(I:C) showed no difference in particle size when compared with naked nanogel. It could be the reason that the aggregation of particles (particle size: 1000 nm) correlated to the diameter size by DLS (figure 8e, 8c and table 1). For the timeline of this TEM imaging, we performed the TEM images after incubation at 30 min and the sample were investigated in the next day.

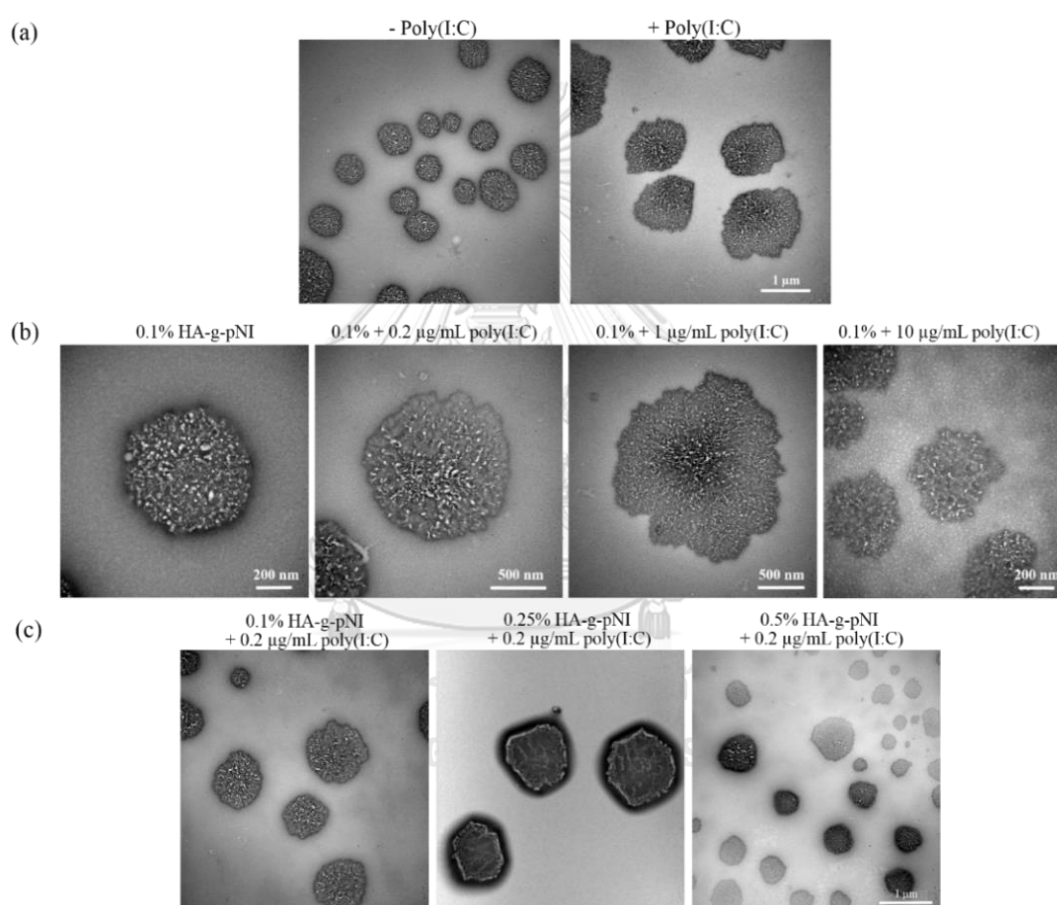


Figure 9 : The particle morphology of assembled HA-g-pNI nanogels with 4% degree of grafting measured by TEM. (a) The comparison between the nanogels without the adjuvant and the nanogels incorporating poly(I:C). (b) Comparison of three different poly(I:C) concentrations loaded in the nanogel formulations. From left to right: 0.1% HA-g-pNI, 0.1% HA-g-pNI loaded 0.2 µg/mL poly(I:C), 0.1% HA-g-pNI loaded 1 µg/mL poly(I:C) and 0.1% HA-g-pNI loaded 10 µg/mL poly(I:C). (c) TEM images of the three

different polymer ratios of nanogel forms loaded with the similarly poly(I:C) amounts. Scale bar shown 1 μm in parts a, and c, and nanoscale level in part b.

V. Evaluation of the lower critical solution temperature of nanogels

Figure 10 showed the similarly thermoresponsive behavior of the blank HA-g-pNI nanogel formulations in each concentration of polymer (% w/v; 0.1, 0.25 and 0.5) with stable dispersion with an aqueous medium. The LCST value of the blank nanogels were close to 35 °C. At below 35 °C, the HA-g-pNI nanoparticles had no significant differences in diameter size range per concentration rise of polymer, at which 0.1% and 0.25% HA-g-pNI had the size in the range of 300-700 nm, and then the size changed abruptly with significant differences of approximately 900-1,000 nm at 35-40 °C. While 0.5% HA-g-pNI started to enlarge up to 2.3 microns with increasing temperature up to 40 °C. These thermoresponsive behaviour can be described that the conversion of the polymeric nanoparticles comprising of the thermoresponsible polymer regions resulted from the hydrophobic effect on the pNIPAM grafting when the temperature over its LCST, causing the change of polymer phase transition and further the particle were swollen. The swelled particles at temperature over LCST of the HA-g-pNI caused by intra-interaction of pNIPAM residues on the HA backbone, which had affected to the expansion of HA chains.

For the thermoresponsive profile of poly(I:C)-loaded nanogels (figure 11) were observed in two nanogel formulations that loaded a poly(I:C) concentration of 0.2 $\mu\text{g/mL}$. There were the small size changing with the poly(I:C) loaded in 0.1% (w/v) HA-g-pNI nanogel in temperature were observed at 34 °C, and then the size started to enlarge up to 400 nm when increasing temperature up to 40 °C, as shown in figure 11. But differed from a formulation of 0.25% (w/v) HA-g-pNI loaded poly(I:C), the average size gradually increases to 900 nm in a diameter. This could be the reason that the decrease of thermoresponsive HA-g-pNI nanogels loaded with a poly(I:C)

macromolecule had affected from the reduction of hydrophobic effect of pNIPAM regions along with the increase of hydrophilicity causing by incorporated the hydrophilic poly(I:C) in the system. From this result, we can utilize the LCST behavior of the polymer for biomedical applications, in particularly drug delivery because it is close to the body temperature. These swelled particles at the temperature above the LCST were believed to the capacity of the expanded circulating time of the nucleic acid in the serum.

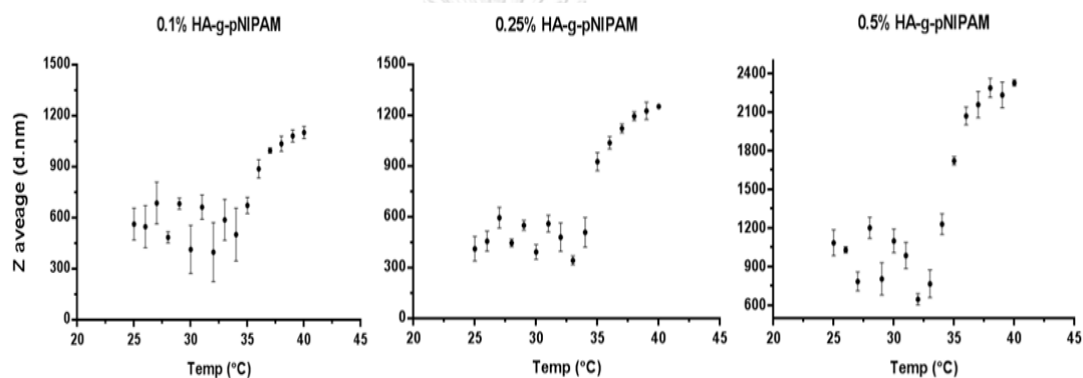


Figure 10 : The LCST profile of naked nanogel in three different concentrations of HA-g-pNI polymer. The experiments were performed by DLS measurement. From left to right: 0.1, 0.25 and 0.5% HA-g-pNIPAM nanogel formulations). The data shown as the mean and standard divisions.

Evaluation of the Lower Critical Solution Temperature of the Poly(I:C)-loaded Nanogels

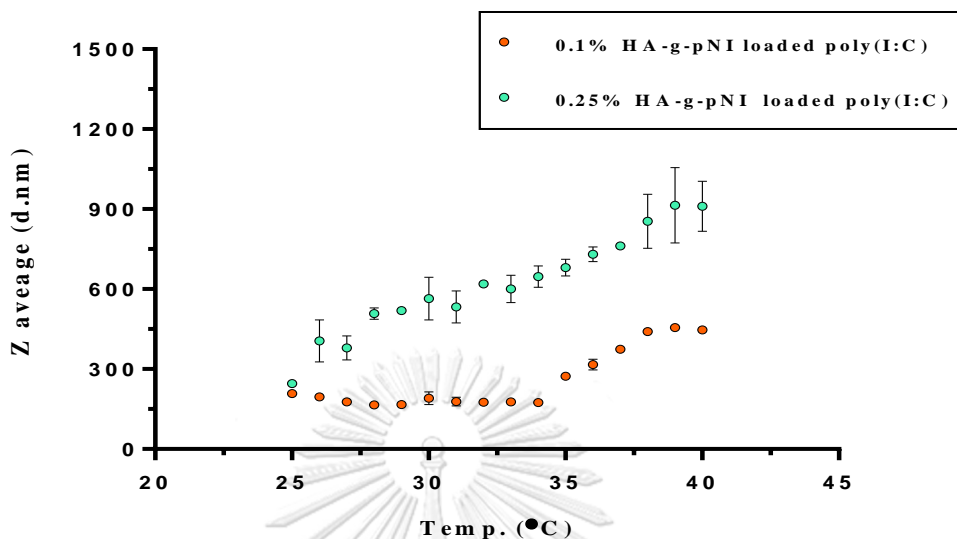


Figure 11 : The LCST profile of poly(I:C)-loaded nanogel formulations in two different concentrations of HA-g-pNI polymer forming gel (% w/v) measured by DLS. The data shown as the mean and standard divisions.

VI. Poly(I:C) formation assessment

To assess that the poly(I:C) association within the HA-g-pNI assembly, all of the poly(I:C) nanogel formulations were incubated with hyaluronidase (A digested enzyme is able to hydrolyze the hyaluronic acid into oligosaccharides) to facilitated poly(I:C) release from the HA-g-pNI nanogel particles. Gel electrophoresis was used to detect the isolated poly(I:C). As shown in figure 12b, the analyzed gel did not detect any bands of the poly(I:C)-incubated hyaluronidase solution compared with the non-treated groups (figure 12a). However, the unexpected event was observed with the soluble poly(I:C)-incubated hyaluronidase as a positive control as seen in figure 12b. Poly(I:C) bands were disappeared after the incubation with hyaluronidase enzyme. This observation could refer to the degradation of poly(I:C) when using hyaluronidase solutions in the experiment, because of the RNase contaminant in the enzyme (55).

Furthermore, electrophoresed gel also demonstrated the recovery amounts of poly(I:C) in the nanogel formulations (in the bottom of figure 12a). The soluble poly(I:C) bands with non-treated hyaluronidase showed the intensity of the band sorted by the poly(I:C) concentrations, a soluble poly(I:C) in concentration of 100 $\mu\text{g}/\text{mL}$ represents the bright band and the brightness decreased from decreasing the poly(I:C) concentrations. The size of poly(I:C) was varied in the range of approximately 1 to 8 kilobases that close to the manufactured size, as indicated in the agarose gel. Afterword, when loaded these concentrations of poly(I:C) into the HA-g-pNI nanogel formulations, we found that the brightness of poly(I:C) nanogel's band (0.1 and 0.25% HA-g-pNI) were close to the unloaded poly(I:C) solutions. Unexpectedly, 0.5% HA-g-pNIPAM formulation with 10 $\mu\text{g}/\text{mL}$ poly(I:C) was not appear its band on the agarose gel. We expected that the poly(I:C) degradation, according to its particle size (measured by DLS) showed no significant differences in the size change compared with the control nanogel (figure 8e and 8f).

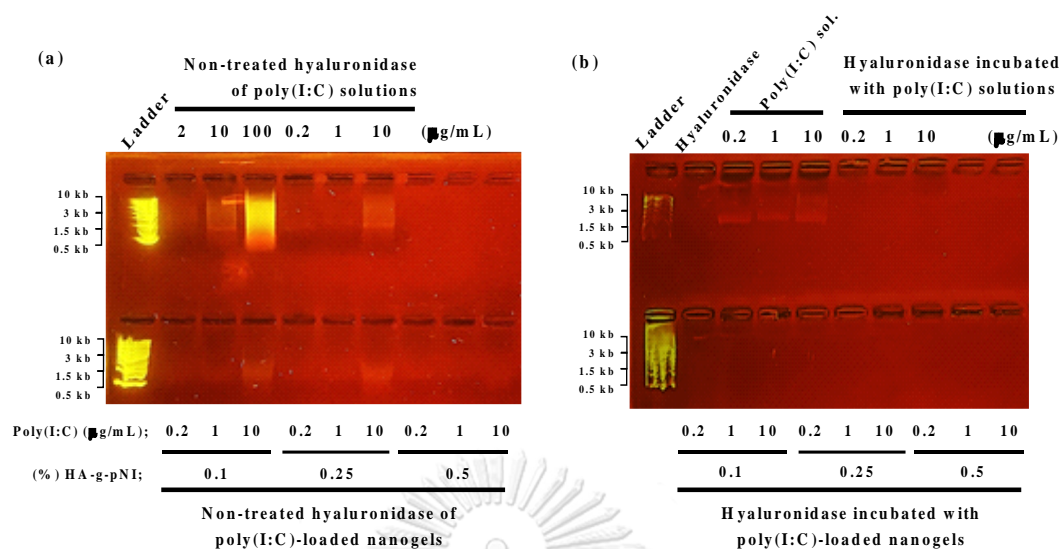


Figure 12 : Agarose gel electrophoresis represents the characteristics of the poly(I:C) incorporated within the HA-g-pNI nanogels in each formulations (a). The poly(I:C) association in the assembled nanogels was evaluated using agarose gel by incubating poly(I:C) nanogel with hyaluronidase solution (b).

VII. Physiological stability of poly(I:C)-loaded HA-g-pNI nanogels against serum degradation

For the evaluation of poly(I:C) stability, nuclease protection assay was performed. The various ratios of poly(I:C) were loaded into the HA-g-pNI nanogels in different concentrations of polymer. The formulations were incubated in the presence of 95% fetal bovine serum (FBS) to evaluate the ability of the carrier system in the protection of poly(I:C) against degradation by nuclease in the serum. Without the nanogel carriers, the bands treated with poly(I:C) alone showed its degradation (<0.5 kb) before 1 h. The complete degradation was observed at 24 hrs (figure 13d). On the other hand, the poly(I:C)-loaded nanogels showed the enhanced stability in the serum demonstrated by the gel electrophoresis. The poly(I:C) formulations that loaded with 0.1% and 0.25% HA-g-pNI showed the bright bands as degraded poly(I:C) at during 6 to 24 hrs, and the poly(I:C) loaded with 0.5% HA-g-pNI had no the band of poly(I:C)

isolates, it was possible that the poly(I:C) RNA interfered with the FBS band. This stability result suggested that HA-g-pNI enhanced the stability as the ratio of the polymer concentration increased (figure 13a, 13b and 13c).

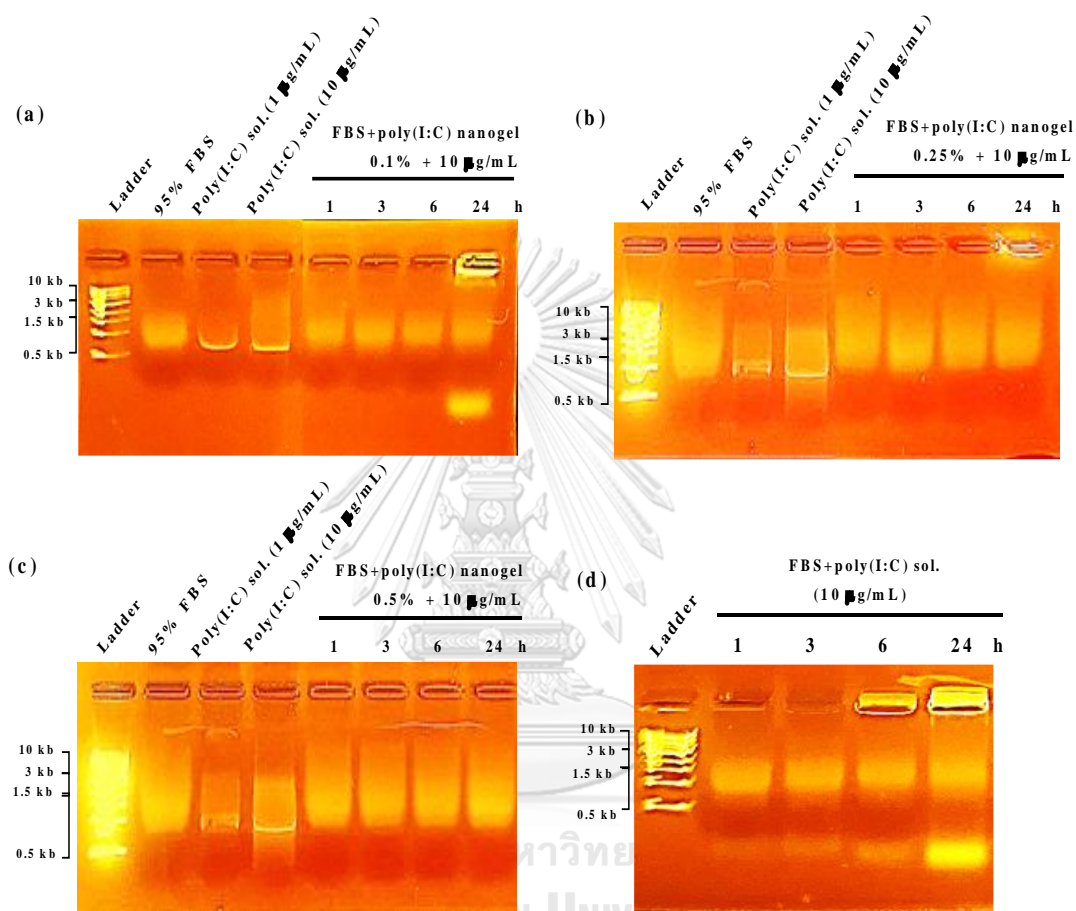


Figure 13 : Comparative gel electrophoresis of the physiological stability of soluble poly(I:C) (d) and poly(I:C)-loaded HA-g-pNI (a, b and c) in the presence of nuclease in FBS.

VIII. Cell viability by RAW 264.7 macrophage cell lines

PrestoBlue® cell viability assay was performed to investigate the cell cytotoxicity of all nanogel formulations through the cell metabolic rate of Resazurin dye. RAW 264.7 murine macrophages were treated for 24 hrs at different formulations of HA-g-pNI nanogels with and without poly(I:C) as well as poly(I:C) solution before subjected

to PrestoBlue assay. As a positive control, untreated cells were set on 100% viable cells. Macrophages exposed to all of the blank nanogel formulations exhibited high viabilities of over 80 % (figure 14a and 14b). It can be reasoned that due to the biocompatible HA backbone within the swelled HA-g-pNI nanogel. With poly(I:C) loading, the cells were prone to the significant decreases of the viability upon the poly(I:C) concentration increase. However, the cell viability was maintained over 80%. In the following study, cells were treated with poly(I:C) solutions at maximum concentrations of 10 and 100 $\mu\text{g}/\text{mL}$, which were well below the threshold for significant loss of cell viability (<80%) (Figure 14c). Thus the use of the soluble poly(I:C) alone led to significant decrease of cell viability compared with the poly(I:C) that incorporated within the HA-g-pNI nanogel carrier. The results demonstrating that there was no significant cytotoxicity among these HA-g-pNI nanogel formulations. They also had a tendency to increase the cell proliferation. Thus, the HA-g-pNI nanogels that loaded with poly(I:C) are a promising candidate for advanced applications with non-cytotoxicity and compatibility as well.

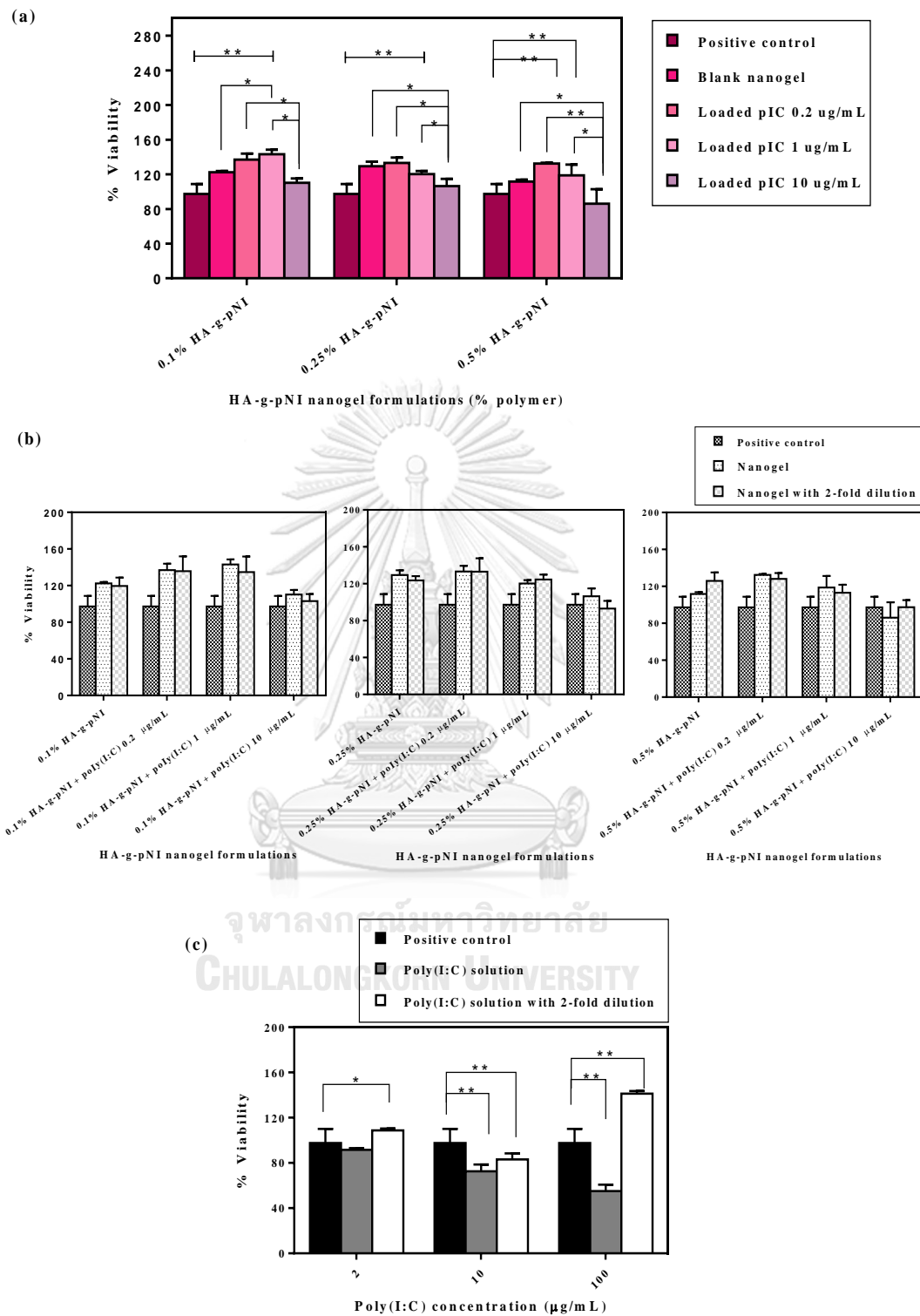


Figure 14 : Viability of RAW 264.7 macrophages treated with different formulations of HA-g-pNI nanogels with and without poly(I:C) (poly(I:C) concentration: 0.2, 1, and 10 µg/mL) as well as comparable poly(I:C) solutions after 24 hrs of incubation for

PrestoBlue[®] assay. **(a)** Comparison of quantitative cell viability between the blank nanogel and poly(l:C)-loaded HA-g-pNI formulations with three different amounts of HA-g-pNI (0.1, 0.25, and 0.5% w/v), **(b)** as well as with 2-fold dilution of these nanogel formulations. **(c)** Cell viability of comparable poly(l:C) solutions in three different concentrations (2, 10, and 100 µg/mL). Untreated cells were used as a positive control (100% viability). The data indicates mean and SEM, and statistic analyse by One-way ANOVA. *p<0.05 and **p<0.01.

IX. The study of cellular uptake of the nanogels

As poly(l:C) exerts its immunostimulatory effects within immune cells, the efficient cell internalization is considered as an essential feature for the treatment in immunotherapy. The cellular uptake study was performed by fluorescence microscope to investigate its qualitative uptake profile of the HA-g-pNI nanogel, which was loaded with the macromolecular poly(l:C) for 24 hrs of incubation. As shown in figure 15, control cells and the cells treated with three different concentrations of blank HA-g-pNI nanogels did not present red fluorescent signal. The cells treated with poly(l:C)-loaded nanogels (poly(l:C), 1 µg/mL) indicated the strong fluorescence showing poly(l:C) accumulation in the cytoplasm and a small increase of the red signal when increasing the nanogel concentrations (% w/v). Furthermore, we observed the improved confluency of the cells via the cell staining experiment when treated with either blank HA-g-pNI nanogels, or poly(l:C)-loaded HA-g-pNI nanogels This observation was in correlation with the cell viability results using PrestoBlue assay as shown in figure 14 (describe below). On the contrary, the fluorescent microscopy of macrophages incubated with a poly(l:C) solution at 1 µg/mL showed less accumulation of poly(l:C). The cells only exhibited strong signal when exposed to higher concentration of soluble poly(l:C) (10 µg/mL).

Relevant to the LCST behaviour, the swollen particle formulations affect the cell

internalization (figure 15). As previously reported findings, one of the key parameter for exhibiting the efficient immunostimulatory effects is the size of particles. Larger particles ($>1 \mu\text{m}$) are phagocytosed by the antigen presenting cells the nano-meter sized particles ($<1 \mu\text{m}$) can be self-taken up by antigen presenting cells; while $<100 \text{ nm}$ in diameter can be internalized as better the big size of particles and self-drain to the lymph nodes (56, 57). Therefore, this nucleic acid carrier system can be potential system to enhance the cell internalization of poly(I:C).



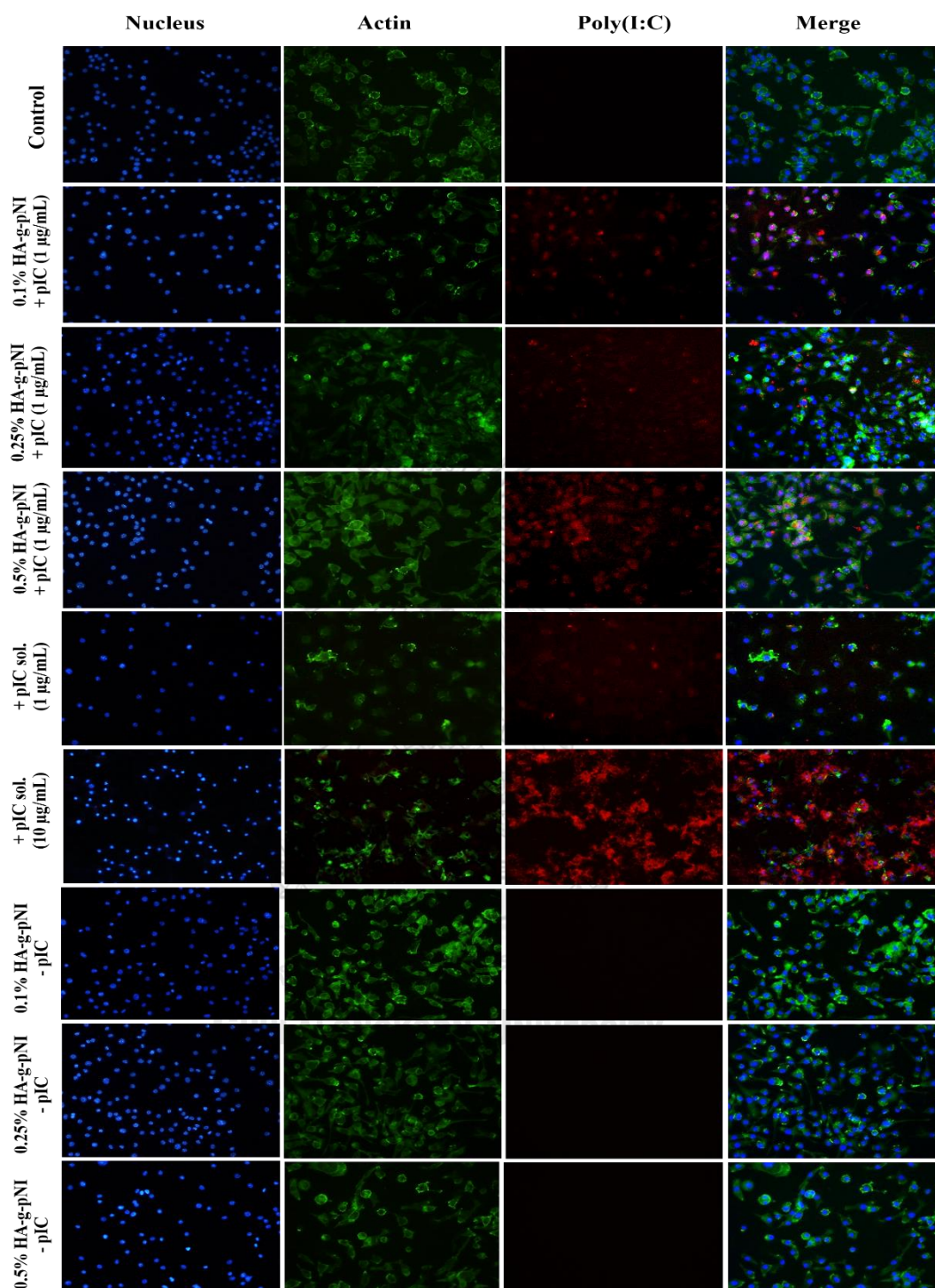


Figure 15 : Cellular uptake study of HA-g-pNI nanogels with- and without poly(I:C) by Raw 264.7 macrophages. Fluorescence images indicating the cellular uptake of nanogels after incubation for 24 hrs. From left to right: DAPI images show the nucleuses; actin green images reveal the cell skeleton; poly(I:C)-tagged rhodamine in red channel ($\lambda_{ex} = 532 \text{ nm}$) indicate its uptake.

CHAPTER V

CONCLUSIONS

In summary, poly(I:C)-loaded biodegradable nanogels were developed and demonstrated for their physical properties following by its biological properties, and biocompatibility of the formulations. The goal of this study was the proof-of concept based on the design and development of the nano-delivery systems by grafting the hyaluronic acid backbone with the thermal sensitive polymer, pNIPAM, for advanced application in incorporation with bioactive compounds to enhance their efficiency. The poly(I:C)-incorporated HA-g-pNI nanogels showed the spherical particles with the diameter size in sub-micron range in water distribution along with the slightly negatively charge on particle surface and LCST profiles in their characteristics. Moreover, the physiological stability of poly(I:C)-loaded nanogel formulations were investigated by nucleus protection assay. Cell-based assay were performed to assess the biological properties (e.g. cellular uptake profile and cell viability test) of the biocompatible nanogel formulations. This systems with loading poly(I:C) were prone to the new generation of vaccine adjuvant as safe and efficient vaccine in therapeutic use.

REFERENCES

1. Mellman I, Coukos G, Dranoff G. Cancer immunotherapy comes of age. *Nature*. 2011;480(7378):480-9.
2. Hafner AM, Corthesy B, Merkle HP. Particulate formulations for the delivery of poly(I:C) as vaccine adjuvant. *Adv Drug Deliv Rev*. 2013;65(10):1386-99.
3. Nordlund JJ, Wolff SM, Levy HB. Inhibition of biologic activity of poly I: poly C by human plasma. *Proc Soc Exp Biol Med*. 1970;133(2):439-44.
4. Foged C, Brodin B, Frokjaer S, Sundblad A. Particle size and surface charge affect particle uptake by human dendritic cells in an in vitro model. *Int J Pharm*. 2005;298(2):315-22.
5. Budhian A, Siegel SJ, Winey KI. Controlling the in vitro release profiles for a system of haloperidol-loaded PLGA nanoparticles. *Int J Pharm*. 2008;346(1-2):151-9.
6. Akira S, Uematsu S, Takeuchi O. Pathogen recognition and innate immunity. *Cell*. 2006;124(4):783-801.
7. Gitlin L, Barchet W, Gilfillan S, Cella M, Beutler B, Flavell RA, et al. Essential role of mda-5 in type I IFN responses to polyriboinosinic:polyribocytidylic acid and encephalomyocarditis picornavirus. *Proc Natl Acad Sci U S A*. 2006;103(22):8459-64.
8. Alexopoulou L, Holt AC, Medzhitov R, Flavell RA. Recognition of double-stranded RNA and activation of NF- κ B by Toll-like receptor 3. *Nature*. 2001;413(6857):732-8.
9. Salmon H, Idoyaga J, Rahman A, Leboeuf M, Remark R, Jordan S, et al. Expansion and Activation of CD103(+) Dendritic Cell Progenitors at the Tumor Site Enhances Tumor Responses to Therapeutic PD-L1 and BRAF Inhibition. *Immunity*. 2016;44(4):924-38.
10. de Clercq E. Degradation of poly(inosinic acid) - poly(cytidylic acid) [(I)n - (C)n] by human plasma. *Eur J Biochem*. 1979;93(1):165-72.
11. Saxena M, Sabado RL, La Mar M, Mohri H, Salazar AM, Dong H, et al. Poly-ICLC, a TLR3 Agonist, Induces Transient Innate Immune Responses in Patients With Treated

HIV-Infection: A Randomized Double-Blinded Placebo Controlled Trial. *Front Immunol.* 2019;10:725.

12. Longhi MP, Trumpfheller C, Idoyaga J, Caskey M, Matos I, Kluger C, et al. Dendritic cells require a systemic type I interferon response to mature and induce CD4+ Th1 immunity with poly IC as adjuvant. *J Exp Med.* 2009;206(7):1589-602.

13. Gale EC, Roth GA, Smith AAA, Alcantara-Hernandez M, Idoyaga J, Appel EA. A Nanoparticle Platform for Improved Potency, Stability, and Adjuvanticity of Poly(I:C). *Adv Ther-Germany.* 2020;3(1).

14. Colapicchioni V, Palchetti S, Pozzi D, Marini ES, Riccioli A, Ziparo E, et al. Killing cancer cells using nanotechnology: novel poly(I:C) loaded liposome-silica hybrid nanoparticles. *J Mater Chem B.* 2015;3(37):7408-16.

15. Rahimian S, Fransen MF, Kleinovink JW, Christensen JR, Amidi M, Hennink WE, et al. Polymeric nanoparticles for co-delivery of synthetic long peptide antigen and poly IC as therapeutic cancer vaccine formulation. *J Control Release.* 2015;203:16-22.

16. DE CLERCQ E. Degradation of Poly(inosinic acid) · poly(cytidylic acid) [(I)n· (C)n] by Human Plasma. *European Journal of Biochemistry.* 1979;93(1):165-72.

17. Oh JK, Siegwart DJ, Lee H-i, Sherwood G, Peteanu L, Hollinger JO, et al. Biodegradable Nanogels Prepared by Atom Transfer Radical Polymerization as Potential Drug Delivery Carriers: Synthesis, Biodegradation, in Vitro Release, and Bioconjugation. *Journal of the American Chemical Society.* 2007;129(18):5939-45.

18. Tahara Y, Akiyoshi K. Current advances in self-assembled nanogel delivery systems for immunotherapy. *Adv Drug Deliv Rev.* 2015;95:65-76.

19. Neamtu I, Rusu AG, Diaconu A, Nita LE, Chiriac AP. Basic concepts and recent advances in nanogels as carriers for medical applications. *Drug Deliv.* 2017;24(1):539-57.

20. Yadav HKS AHN, Alsalloum GA. Nanogels as novel drug delivery systems - a review. *J Pharm Pharm Res.* 2017;1:5.

21. Robert Langer NAP. Advances in Biomaterials, Drug Delivery, and Bionanotechnology. *AIChE Journal.* 2003;49:42.

22. Kandil R, Merkel OM. Recent Progress of Polymeric Nanogels for Gene Delivery. *Curr Opin Colloid Interface Sci.* 2019;39:11-23.
23. Oh JK, Siegwart DJ, Lee HI, Sherwood G, Peteanu L, Hollinger JO, et al. Biodegradable nanogels prepared by atom transfer radical polymerization as potential drug delivery carriers: synthesis, biodegradation, in vitro release, and bioconjugation. *J Am Chem Soc.* 2007;129(18):5939-45.
24. Li D, van Nostrum CF, Mastrobattista E, Vermonden T, Hennink WE. Nanogels for intracellular delivery of biotherapeutics. *J Control Release.* 2017;259:16-28.
25. Alexopoulou L, Holt, A., Medzhitov, R. et al. Recognition of double-stranded RNA and activation of NF- κ B by Toll-like receptor 3. *Nature.* 2001;413:732-8.
26. Li D, Sun F, Bourajaj M, Chen Y, Pieters EH, Chen J, et al. Strong in vivo antitumor responses induced by an antigen immobilized in nanogels via reducible bonds. *Nanoscale.* 2016;8(47):19592-604.
27. Han HD, Byeon Y, Jang JH, Jeon HN, Kim GH, Kim MG, et al. In vivo stepwise immunomodulation using chitosan nanoparticles as a platform nanotechnology for cancer immunotherapy. *Sci Rep.* 2016;6:38348.
28. Kogan G, Soltés L, Stern R, Gemeiner P. Hyaluronic acid: a natural biopolymer with a broad range of biomedical and industrial applications. *Biotechnol Lett.* 2007;29(1):17-25.
29. YARON. M, YARON., SMETANA., EYLAN. E, . MH. <HYALURONIC ACID PRODUCED BY fibroblast _effect of poly IC.pdf>. *Arthritis and Rheumatism.* 1976;19:6.
30. Rapport MM, Weissmann B, Linker A, Meyer K. Isolation of a crystalline disaccharide, hyalobiuronic acid, from hyaluronic acid. *Nature.* 1951;168(4284):996-7.
31. Khunmanee S, Jeong Y, Park H. Crosslinking method of hyaluronic-based hydrogel for biomedical applications. *J Tissue Eng.* 2017;8:2041731417726464.
32. Mattheolabakis G, Milane L, Singh A, Amiji MM. Hyaluronic acid targeting of CD44 for cancer therapy: from receptor biology to nanomedicine. *Journal of Drug Targeting.* 2015;23(7-8):605-18.
33. Johnson P, Arif AA, Lee-Sayer SSM, Dong Y. Hyaluronan and Its Interactions With Immune Cells in the Healthy and Inflamed Lung. *Frontiers in Immunology.* 2018;9(2787).

34. Pedrosa SS, Pereira P, Correia A, Gama FM. Targetability of hyaluronic acid nanogel to cancer cells: In vitro and in vivo studies. *Eur J Pharm Sci.* 2017;104:102-13.
35. Penno MB, August JT, Baylin SB, Mabry M, Linnoila RI, Lee VS, et al. Expression of CD44 in human lung tumors. *Cancer Res.* 1994;54(5):1381-7.
36. Knudson W, Chow G, Knudson CB. CD44-mediated uptake and degradation of hyaluronan. *Matrix Biol.* 2002;21(1):15-23.
37. Fernandes Stefanello T, Szarpak-Jankowska A, Appaix F, Louage B, Hamard L, De Geest BG, et al. Thermoresponsive hyaluronic acid nanogels as hydrophobic drug carrier to macrophages. *Acta Biomater.* 2014;10(11):4750-8.
38. Wei X, Senanayake TH, Warren G, Vinogradov SV. Hyaluronic acid-based nanogel-drug conjugates with enhanced anticancer activity designed for the targeting of CD44-positive and drug-resistant tumors. *Bioconj Chem.* 2013;24(4):658-68.
39. Lee H, Mok H, Lee S, Oh YK, Park TG. Target-specific intracellular delivery of siRNA using degradable hyaluronic acid nanogels. *J Control Release.* 2007;119(2):245-52.
40. Kita R, Kircher G, Wiegand S. Thermally induced sign change of Soret coefficient for dilute and semidilute solutions of poly(N-isopropylacrylamide) in ethanol. *J Chem Phys.* 2004;121(18):9140-6.
41. Okada Y, Tanaka F. Cooperative hydration, chain collapse, and flat LCST behavior in aqueous poly(N-isopropylacrylamide) solutions. *Macromolecules.* 2005;38(10):4465-71.
42. Kujawa P, Aseyev V, Tenhu H, Winnik FM. Temperature-Sensitive Properties of Poly(N-isopropylacrylamide) Mesoglobules Formed in Dilute Aqueous Solutions Heated above Their Demixing Point. *Macromolecules.* 2006;39(22):7686-93.
43. Yang HW, Lee AW, Huang CH, Chen JK. Characterization of poly(N-isopropylacrylamide)-nucleobase supramolecular complexes featuring bio-multiple hydrogen bonds. *Soft Matter.* 2014;10(41):8330-40.
44. Yoshida R, Uchida K, Kaneko Y, Sakai K, Kikuchi A, Sakurai Y, et al. Comb-type grafted hydrogels with rapid deswelling response to temperature changes. *Nature.* 1995;374(6519):240-2.

45. Huffman AS, Afrassiabi A, Dong LC. Thermally reversible hydrogels: II. Delivery and selective removal of substances from aqueous solutions. *Journal of Controlled Release*. 1986;4(3):213-22.
46. Chen G, Hoffman AS. Graft copolymers that exhibit temperature-induced phase transitions over a wide range of pH. *Nature*. 1995;373(6509):49-52.
47. Luckanagul JA, Pitakchatwong C, Ratnatilaka Na Bhuket P, Muangnoi C, Rojsitthisak P, Chirachanchai S, et al. Chitosan-based polymer hybrids for thermo-responsive nanogel delivery of curcumin. *Carbohydr Polym*. 2018;181:1119-27.
48. Chen J, Wu M, Veroniaina H, Mukhopadhyay S, Li J, Wu Z, et al. Poly(N-isopropylacrylamide) derived nanogels demonstrated thermosensitive self-assembly and GSH-triggered drug release for efficient tumor Therapy. *Polymer Chemistry*. 2019;10(29):4031-41.
49. D'Este M, Alini M, Eglin D. Single step synthesis and characterization of thermoresponsive hyaluronan hydrogels. *Carbohydr Polym*. 2012;90(3):1378-85.
50. D'Este M, Alini M, Eglin D. Single step synthesis and characterization of thermoresponsive hyaluronan hydrogels. *Carbohydrate polymers*. 2012;90(3):1378-85.
51. D'Este M, Eglin D, Alini M. A systematic analysis of DMTMM vs EDC/NHS for ligation of amines to hyaluronan in water. *Carbohydrate polymers*. 2014;108:239-46.
52. Kim JH, Moon MJ, Kim DY, Heo SH, Jeong YY. Hyaluronic Acid-Based Nanomaterials for Cancer Therapy. *Polymers-Basel*. 2018;10(10).
53. Zhang XJ, Achazi K, Steinhilber D, Kratz F, Deredde J, Haag R. A facile approach for dual-responsive prodrug nanogels based on dendritic polyglycerols with minimal leaching. *Journal of Controlled Release*. 2014;174:209-16.
54. Jeon S, Clavadetscher J, Lee DK, Chankeshwara SV, Bradley M, Cho WS. Surface Charge-Dependent Cellular Uptake of Polystyrene Nanoparticles. *Nanomaterials (Basel)*. 2018;8(12).
55. Robert Love RHL, and Kay A. O. Ellem. Activity of Ribonuclease in Preparations of Testicular and Streptococcal Hyaluronidase. *J histochem Cytochem*. 1960;8:437-41.
56. Howard GP, Verma G, Ke X, Thayer WM, Hamerly T, Baxter VK, et al. Critical size limit of biodegradable nanoparticles for enhanced lymph node trafficking and paracortex penetration. *Nano Research*. 2019;12(4):837-44.

57. Lunov O, Syrovets T, Loos C, Beil J, Delacher M, Tron K, et al. Differential uptake of functionalized polystyrene nanoparticles by human macrophages and a monocytic cell line. *ACS Nano*. 2011;5(3):1657-69.



REFERENCES



จุฬาลงกรณ์มหาวิทยาลัย
CHULALONGKORN UNIVERSITY



จุฬาลงกรณ์มหาวิทยาลัย
CHULALONGKORN UNIVERSITY

VITA

NAME Nararat Kotcharat

DATE OF BIRTH 12th April 1995

PLACE OF BIRTH Chonburi, Thailand

INSTITUTIONS ATTENDED Bachelor of Science in medical sciences, 2018, Huachiew Chalermprakiet University, Thailand.

HOME ADDRESS 4 m.4 Samaesan, Sattahip, Chonburi, 20180, Thailand

PUBLICATION Nararat Kotcharat, Penpimol Charoenkanburkang, Jittima Amie Luckanagul. Grafted Hyaluronic Acid Nanogel for the Incorporation of Poly(I:C) as an Immunostimulatory Adjuvant. SRP. (2020); 11(11): 247-253.
doi:10.31838/srp.2020.11.36

AWARD RECEIVED -